# Master 2 Internship

# Approximation schemes for the glass transition in simple systems

# MANGEAT Matthieu - matthieu.mangeat@ens.fr

April 10th, 2015

Laboratoire de Physique Théorique de l'Ecole Normale Supérieure - Paris From January 12h to March 6th, 2015 Internship supervisor : ZAMPONI Francesco - francesco.zamponi@corto.lpt.ens.fr ENS correspondant : BILAL Adel - adel.bilal@corto.lpt.ens.fr

Table of Contents				2.1 The replicated entropy	7
_				2.2 The equation for A	8
				2.3 The complexity	9
1	Some generalities about liquids and glasses			2.4 The equilibrium equations $(\varphi_d, \varphi_K)$	9
	1.1 Theory of liquids	. 2		2.5 The jamming equations $(\varphi_{th}, \varphi_{GCP})$	9
	1.1.1 Some definitions		3	Dimensional behaviour of the phase diagram	10
	<b>1</b>			3.1 Asymptotic behaviour	10
	1.1.3 The direct correlation function $c(r)$			3.1.1 Derivation of $q_A(r)$	10
	1.1.4 The HNC approximation			3.1.2 Derivation of $S_{liq}(\varphi)$	11
	1.1.5 The PY approximation			3.1.3 Derivation of densities	11
	1.1.6 The CS approximation			3.2 Small cage expansion	12
	1.1.7 The VW approximation			3.2.1 Derivation of $\Sigma_{eq}$ and $\varphi_K$	12
	1.2 Generalities about glasses			3.2.2 Derivation of $\Sigma_j$ and $\varphi_{GCP}$	13
	1.2.1 The relaxation time $\dots$	. 5		3.3 Computation for finite dimension	13
	1.2.2 The phase diagram of glasses	. 6		3.3.1 Algorithm for $g_{liq}(r,\varphi)$	13
	1.2.3 The replica method	. 6		3.3.2 Algorithm to compute the densities	15
		_		3.3.3 Numerical results for densities	16
<b>2</b>	Derivation of equations for the entropy and	the			
	nhase diagram	7	4	The non-ergodicity factor	18

# Introduction

During my internship, I dealt with the glass transition, an important problem because the glassy state exists everywhere in the matter but there is no theory universally accepted about this state. On the technical aspect, the difficulties come from the phase transition in presence of disorder and the multiplicity of metastable states.

Many statistical mechanics models are exactly solvable in infinite spatial dimensions. The exact solution has a mean field structure, and a systematic 1/d expansion around this solution can be obtained in the form of a high temperature/low density expansion. Examples are the Ising model of magnetic materials, which is described by the Curie-Weiss mean field theory for  $d=\infty$ , and a hard sphere liquid, which is described by the Van der Waals equation of state.

For the glass transition problem, this strategy can be applied to a prototypical glass former, namely hard spheres. The phase diagram turns out to be similar to the one of a class of spin glass models (*p*-spin and Potts glasses), thus confirming the general picture of the Random First Order Transition theory of the glass transition.

The striking difference with respect to ordinary phase transitions is that the glass phase is not a unique phase (like, e.g. a crystal). In the glassy region of the phase diagram, multiple distinct glass states appear, each characterized by different thermodynamic properties (e.g. a different equation of state). The glassy phase diagram is thus extremely complex and characterized by several distinct phase transitions.

The natural question once the  $d=\infty$  solution has been constructed, is to include finite dimensional corrections in a controlled way. Our approach consists of including quantitative finite dimensional corrections by perturbations, using the theory of liquids and the replica method explained in the first section. In fact, in  $d=\infty$  typically only a few diagrams of the high temperature/low density expansion are relevant. In finite dimensions, instead, all the diagrams of the expansion contribute. Including a certain number (or even an infinite class) of diagrams typically does not change the qualitative phase diagram of the system, which remains the same as in  $d=\infty$ , but changes the quantitative results for all the physical quantities (e.g. the transition temperature/density, or the specific heat). Away from the critical region around a phase transition, the inclusion of a few diagrams gives already quite good results for the Ising model.

For particle systems, resummation of classes of diagrams are needed, leading to the successful approximations schemes of standard liquid theory, like the Hypernetted Chain (HNC) or Percus-Yevick (PY) approximations.

The calculation of the phase diagram is thus possible in the approach we developed at all dimensions whereas the previous approaches only gave some parts of the diagram. The main calculation of the important transition point of phase diagram is done in the second section after the perturbative derivation. The previous approaches are coherent with our approach as shown in the beginning of section 3. At the end of the third section, the numerical results of equations derived in the second one will be presented. Finally, in section 4, the derivation of the non-ergodicity factor will be done in our approach, which could not be done in the previous approaches.

# 1 Some generalities about liquids and glasses

In this section, I will present some results and derivations needed all along my internship about, first, the theory of liquids and secondly, about the glass transition, its phase diagram and the useful replica method.

# 1.1 Theory of liquids

#### 1.1.1 Some definitions

We consider the liquid as an ensemble of N molecules of size  $\sigma=1$  which interact with a potential v(r) in an external field  $\Psi(r)$ . This potential can be described by different models more or less sophisticated: hard-sphere, square-well, Yukawa, Lennard-Jones potentials for example. We will consider, for this section, a general form of v(r) and next, we will be interested only in the simplest one: the hard-sphere potential

$$v_{HS}(r) = \begin{cases} \infty & r < \sigma \\ 0 & r > \sigma \end{cases}$$
 (1.1.1)

The partition function can be written in the grand-canonical ensemble as

$$Z_N = \frac{1}{N!} e^{N\beta\mu} \int dr_1 ... dr_N \exp\left[-\beta \left(\sum_{i=1}^N \sum_{j=1}^{i-1} v(r_i - r_j) - \sum_{i=1}^N \Psi_i\right)\right]$$
(1.1.2)

We define the n-point correlation functions, also called the n particle densities, as

$$\rho_N^{(n)}(r_1,...,r_n) = \frac{N!}{(N-n)!} \frac{1}{Z_N} \int dr_{n+1}...dr_N \exp\left[-\beta \left(\sum_{i=1}^N \sum_{j=1}^{i-1} v(r_i - r_j) - \sum_{i=1}^N \Psi_i\right)\right] = \langle \sum_{i_1 \neq ... \neq i_n} \delta(r_1 - r_{i_1})...\delta(r_n - r_{i_n})\rangle$$
(1.1.3)

and the pair correlation

$$g_N^{(n)}(r_1, ..., r_n) = \rho^{-n} \rho_N^{(n)}(r_1, ..., r_n), \quad h_N^{(n)}(r_1, ..., r_n) = g_N^{(n)}(r_1, ..., r_n) - 1$$
(1.1.4)

In the following we mostly use  $\rho_N^{(1)}(r_1) \equiv \rho_1 \equiv \rho(r)$ ,  $\rho_N^{(2)}(r_1, r_2) \equiv \rho_{12} \equiv \rho_{12}^{(2)}(r)$ ,  $g_N^{(2)}(r_1, r_2) \equiv g_{12} \equiv g(r)$  and  $h_N^{(2)}(r_1, r_2) \equiv h_{12} \equiv h(r)$ . The density of the liquid will be denoted  $\rho = \langle \rho(r) \rangle$  and the packing fraction  $\varphi = V_d(\frac{1}{2})\rho = \frac{\pi^{\frac{d}{2}}\rho}{2^d\Gamma(\frac{d}{2}-1)}$ , where  $V_d(R)$  is the volume of the d-dimension hypersphere of radius R.

We can finally define the structure factor as  $S(k) = \langle \frac{1}{N} \rho(k) \rho(-k) \rangle = 1 + \rho \int dr h(r) e^{-ikr}$  which is the pair correlation's Fourier transform.

#### 1.1.2 The partition function

The derivation of the partition function, from a diagrammatic way, is well done in [HM76, Jac13]. Some steps of this derivation are reproduced here for a better comprehension of the result and the different approximations. We use a handy notation :  $\int dr_1 \equiv \int d1$ ,  $F(r_1, r_2) \equiv F_{12}$  for all functions and for the diagrams, we consider a white node  $\circ$  as a constant equal to 1 without integration, a black node  $\bullet$  as  $\int d1z_1$  such that  $z_1 = e^{\beta(\mu - \Psi_1)} = e^{\nu_1}$  and a line — as  $f_{12} = e^{-\beta v_{12}} - 1 = e^{w_{12}} - 1$ , the Mayer function. Writing only the contribution with 0, 1, 2 and 3 nodes, the partition function reduces as,

The logarithm of Z, the only function we need to calculate the entropy, reduces to the connected diagrams. We get at the order 3 in f,

We introduce then a first Legendre transformation as

$$\Gamma_1[\rho, w] = \log Z[\nu^*, w] - \int d1\nu_1^* \rho_1, \quad \frac{\delta \log Z}{\delta \nu_1} \Big|_{\nu_1^*} = \rho_1$$
 (1.1.7)

Taking the functional derivative of  $\log Z$  with respect to  $z_1$ , i.e. replacing one black node by a white node, we get

Taking the logarithm of this expression, i.e. only the diagrams whose the black node chain is connected, we get

$$\nu_1 = \log \rho_1 - \Theta - \mathcal{O} - \mathcal{O} - \mathcal{O} - \mathcal{O} + \mathcal{O}(f^4)$$

$$(1.1.9)$$

Now, we change the variable z, from the equation (1.1.8). The black nodes represent now  $\rho[\nu]$  and white nodes a constant equal to 1.

$$\nu_1^* = -\frac{\delta \Gamma_1[\rho, w]}{\delta \rho_1} = \log \rho_1 - \bigcirc - \bigcirc + \mathcal{O}(f^4)$$
(1.1.10)

By integrating, we get then

This is the so-called Virial expansion of the liquid theory where  $\int d1\rho_1(1-\log\rho_1)$  corresponds to the ideal gas. The only diagrams of  $\rho$  nodes and f lines are connected one particle irreducible diagrams. We will perform now a second Legendre transformation

$$\Gamma_2[\rho, \rho^{(2)}] = \Gamma_1[\rho, w^*] - \frac{1}{2} \int d1 d2 w_{12}^* \rho_{12}^{(2)}, \quad \frac{\Gamma_1[\rho, w]}{\delta w_{12}^*} \Big|_{w_{12}^*} = \frac{1}{2} \rho_{12}^{(2)}$$
(1.1.12)

The two point correlation, using previous rules and the fact that the division by  $\rho$  replaces a black node by a white one, is given by

$$g_{12} = \frac{\rho_{12}^{(2)}}{\rho_1 \rho_2} = \frac{2}{\rho_1 \rho_2} (1 + f_{12}) \frac{\delta \Gamma_1^{ex}[\rho, w]}{\delta f_{12}} = e^{w_{12}} (1 + \rho_0 + \rho$$

Taking the logarithm, we get

$$w_{12} = \log(1 + h_{12}) - 2 - \sqrt{1 - \frac{1}{\sqrt{3}}} - \sqrt{1 - \frac{1}{\sqrt{3}}} + \mathcal{O}(\rho^3)$$
(1.1.14)

Now, to perform the Legendre transformation, we replace the lines of f by lines of h using the equation (1.1.13), we get

$$h_{12} = f_{12} + \mathcal{O} + \mathcal{O$$

$$w_{12}^* = \frac{\delta\Gamma_2[\rho, \rho^{(2)}]}{\delta\rho^{(2)}} = -\frac{2}{\rho_1\rho_2} \frac{\delta\Gamma_2[\rho, \rho^{(2)}]}{\delta h_{12}} = \log(1 + h_{12}) - \bigcirc -\bigcirc -\bigcirc -\bigcirc -\bigcirc +\bigcirc + \mathcal{O}(\rho^3)$$
(1.1.16)

By integrating, we get then the Morita and Hiroike functional,

$$\Gamma_2[\rho, \rho^{(2)}] = \int d1\rho_1(1 - \log \rho_1) + \frac{1}{2} \int d1d2\rho_1\rho_2[h_{12} - (1 + h_{12}) \cdot \log(1 + h_{12})] + A - \Box + \Box + \Box + \mathcal{O}(\rho^5)$$
(1.1.17)

$$\Gamma_{2}[\rho, \rho^{(2)}] = \int d1\rho_{1}(1 - \log \rho_{1}) + \frac{1}{2} \int d1d2\rho_{1}\rho_{2}[h_{12} - (1 + h_{12}) \cdot \log(1 + h_{12})] + A - + \{\text{other ring diagrams}\} + \{2\text{PI diagrams}\}$$
(1.1.18)

# 1.1.3 The direct correlation function c(r)

We can also get by definition, the direct correlation from the Virial expansion,

From the equations (1.1.15) and (1.1.16), we get

$$w_{12}^* = \log(1 + h_{12}) - h_{12} + c_{12} + \{\text{a class of diagrams}\}$$
(1.1.20)

This equation can be solved iteratively . We get at the first order

$$c(r) = h(r) - \rho \int dr' h(r - r') c(r') \Rightarrow \hat{h}(k) = \frac{\hat{c}(k)}{1 - \rho \hat{c}(k)}$$
(1.1.21)

which is the so-called Ornstein-Zernike equation, which says that h-c is the convolution of c with  $\rho h$ . At the next orders,

#### The Hyper-Netted-Chain (HNC) approximation

The HNC approximation consists in removing all two particle irreducible diagrams. From this, we get the HNC equation

$$c(r) = e^{w(r)}e^{h(r)-c(r)} - 1 - [h(r) - c(r)]$$
 (1.1.23) from the  $w^*$  equation, removing the class of diagrams. From the equation of  $\Gamma_2$ , we get the expression of the entropy

$$S[\rho, h] = \frac{1}{N} \log Z[\nu, w] = \frac{1}{N} \Gamma_1[\rho, w] = \frac{1}{N} \Gamma_2[\rho, h] + \frac{1}{2N} \int d1 d2 w_{12} \rho_1 \rho_2 (1 + h_{12})$$
(1.1.24)

$$S[\rho, g] = \frac{1}{N} \int dr \rho(r) [1 - \log \rho(r)] - \frac{1}{2N} \int dr_1 dr_2 \rho(r_1) \rho(r_2) \{g(r_1, r_2) [\log g(r_1, r_2) + \beta v(r_1, r_2) - 1] + 1\}$$

$$+ \frac{1}{2N} \sum_{n \ge 3} \frac{(-1)^n}{n} Tr_x [\rho h]^n$$
(1.1.25)

where  $Tr_x[\rho h]^n$  is nothing else that the n side ring diagram.

### The Percus-Yevick (PY) approximation

The Percus-Yevick approximation consists to consider that |c-h| is small in the HNC approximation, we get thus

$$c(r) = [1 - e^{-w(r)}] \cdot [1 + h(r)] \Rightarrow c(r) = e^{w(r)} \cdot [1 + h(r) - c(r)] - 1 - [h(r) - c(r)]$$
(1.1.26)

This approximation is better than the HNC approximation for the pair correlation but worse for the entropy which is obtained using the equation (1.1.29) for the Percus-Yevick pair correlation.

#### The Carnahan-Starling (CS) approximation 1.1.6

In this approximation, we consider only the first three terms of the Virial expansion to calculate the entropy therefore. The reduced pressure is

$$p = 1 + 2^{d-1}\varphi g(1,\varphi), \quad g(1,\varphi) = \frac{1 - \mathcal{A}_d \varphi}{(1-\varphi)^d}$$
 (1.1.27)

where  $\varphi$  is the packing fraction and  $\mathcal{A}_d$  is defined in terms of the second (b) and third (B<sub>3</sub>) Virial terms defined in [SMS89]

$$\mathcal{A}_d = d - 2^{d-1} \frac{B_3}{b^2}, \quad \frac{B_3}{b^2} = 2 \left[ 1 - \frac{\Gamma(1 + \frac{d}{2})}{\Gamma(\frac{1}{2})\Gamma(\frac{d+1}{2})} \right] {}_{2}F_{1} \left[ \frac{1}{2}, \frac{1-d}{2}; \frac{3}{2}; \frac{1}{4} \right]$$

$$(1.1.28)$$

where  ${}_2F_1$  is the hypergeometric function. Some other values of  $\mathcal{A}_d$  are obtained in [CIPZ11] by numerical simulations of the equation of state. From this we can easily get the entropy as

$$p = -\varphi \frac{\partial S}{\partial \varphi}$$
 and  $S(\varphi = 0) \sim 1 - \log \rho \Rightarrow S(\varphi) = 1 - \log \rho - 2^{d-1} \int_0^{\varphi} d\varphi' g(1, \varphi')$  (1.1.29)

where  $S(\varphi = 0)$  is the ideal gas behaviour. We get thus

$$S(\varphi) = 1 - \log \rho - \frac{2^{d-1}}{(d-1)(1-\varphi)^{d-1}} \left\{ \frac{\mathcal{A}_d}{d-2} \left[ (1-\varphi)^{d-1} - 1 + \varphi(d-1) \right] + (1-\varphi)^{d-1} - 1 \right\}$$
(1.1.30)

This particular factorization will be useful for a numerical evaluation of the entropy for small  $\varphi$ . From this particular value of g(1), a new approximation can be derived for g(r) in the special case of dimension 3 (Sec. 1.1.7), but no generalization exists for other dimensions.

# The Verlet-Weis (VW) approximation

This approximation consists to fit as well as possible the pair correlation obtained by computer "experiments" modifying the Percus-Yevick solution, done in [VW72, HM76]. The solution is taken to have  $g_{VW}(1) = g_{CS}(1)$  given by (1.1.27) and to give a phase shift such that

$$g_{VW}(r,\varphi) = g_{PY}(\xi r, \varphi^*) + \delta g(r)$$

$$\delta g(r) = \frac{\delta g_1}{r} \cos[\alpha(r-1)]e^{-\alpha(r-1)}$$
(1.1.31)

with in dimension 3, the parameters  $\varphi^* = \varphi - \frac{\varphi^2}{16}$ ,  $\xi = \left(\frac{\varphi}{\varphi^*}\right)^{1/3}$ ,  $\delta g_1 = g_{CS}(1) - g_{PY}(\xi)$  and  $\alpha = \frac{24\delta g_1}{\varphi^* g_{PY}(1)}$ .  $\varphi^*$  is chosen to achieve a minimum in the absolute difference between the exact function and  $g_{PY}$ ,  $\delta g_1$  to fit the Carnahan-Starling equation and  $\alpha$  to obtain the correct isothermal compressibility. This result fits the exact computer-generated function with an error less than 1% for all  $\varphi$ .

We try to generalize this, with the same form of g and new values for  $\alpha = \frac{24\delta g_1}{\varphi^{*3/d}g_{PY}(1)}$  and  $\xi = \left(\frac{\varphi}{\varphi^*}\right)^{1/d}$ , which is coherent with the d=3 solution. The behaviour of this solution seems to be good but it is maybe unexact.

# 1.2 Generalities about glasses

The glassy state of matter is omnipresent in daily life. It is obtained by cooling a liquid with a fast quench under the glass temperature  $T_g$  defined as the temperature where the relaxation time and thus the viscosity exceeds any reasonable human timescales.  $T_g$  is defined from the viscosity  $\eta(T_g) \sim 10^{12}$  Pa.s or the relaxation time  $\tau_{\alpha}(T_g) \sim 100$ s. To have this state of the matter, out-of-equilibrium, the crystal must not be formed, in fact, during a fast quench, the nucleation of the crystal is not thermodynamically favorable. Below  $T_g$ , due to the viscosity, any nucleation is stopped. The glass is a frozen liquid and thus conserves its static properties, like e.g. the pair correlation g(r).

#### 1.2.1 The relaxation time

With the notations of section 1.1, we can define the mean-square displacement  $\Delta$  and the diffusivity D of the liquid as

$$\Delta(t) = \langle \frac{1}{N} \sum_{i=1}^{N} |r_i(t) - r_i(0)|^2 \rangle, \quad D = \lim_{t \to \infty} \frac{\Delta(t)}{2dt}$$
 (1.2.1)

As explained in [BB11, Cav09], the relaxation of a glass happens in two steps :

- 1. a relaxation  $\beta$  fast which relaxes the ballistic regime to a localized regime where  $\Delta$  reaches a plateau (D=0),
- 2. a relaxation  $\alpha$  slow which relaxes the localized regime to a diffusive regime.

For a liquid, there is only a fast relaxation from a ballistic regime to a diffusive regime. The relaxation time of  $\alpha$  is characteristic of a glass and large compare to the daily timescale.

The relaxation time  $\tau_{\alpha}$  of the glass can be fitted by different kind of laws as function of the temperature.

A strong glass-former (e.g.  $SiO_2$ ,  $GeO_2$ ) has the relaxation time which follows a purely Arrhenius law

$$\tau_{\alpha} = \tau_0 e^{\beta E} \tag{1.2.2}$$

A fragile glass-former (e.g. toluene, o-therphenyl) has a relaxation time which follows a super-Arrhenius behaviour characterized by a Vogel-Fulcher-Tamman law

$$\tau_{\alpha} = \tau_0 \exp\left(\frac{DT_g}{T - T_g}\right) \tag{1.2.3}$$

This behaviour can be also fitted by a double Arrhenius law, with different parameters, into the two domains  $T \ll T_g$  and  $T \sim T_g$ .

Some other laws can exist, the Bässler law

$$\tau_{\alpha} = \tau_0 \exp\left[K\left(\frac{T_*}{T}\right)^2\right] \tag{1.2.4}$$

or another law replacing 1/T by  $1/T-1/T_{on}$  in the Bässler law to have a divergence at  $T \neq 0$ .

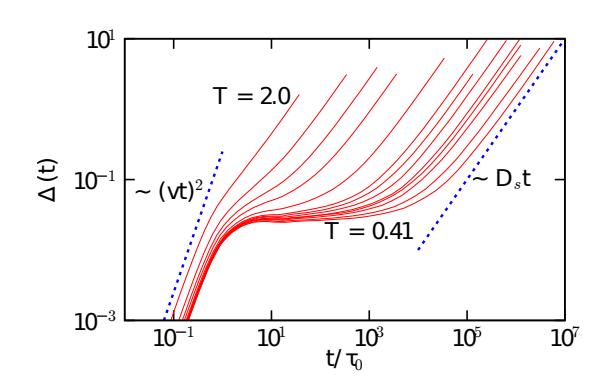


FIGURE 1 – Mean-square displacement of individual particles of a glass-forming liquid for different temperature (Figure from [BB11]).

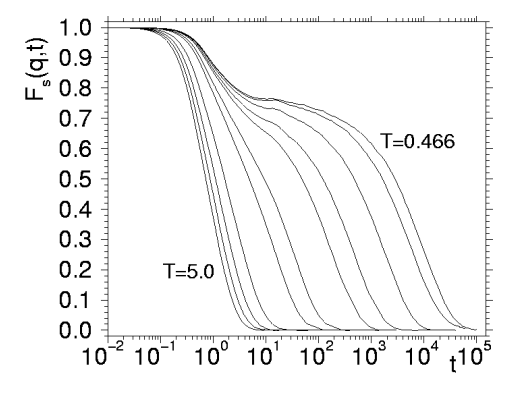


FIGURE 2 – The two-steps relaxation in the scattering function  $F_s(q,t)$ . The behaviour is exponential at high temperature (Figure from [Cav09]).

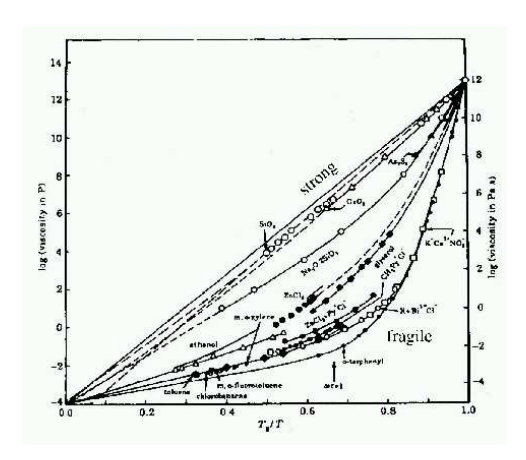


FIGURE 3 – Logarithm of the viscosity vs. the inverse temperature  $T_g/T$ , which represents the behaviour of relaxation time of liquids close to the glass transition (Figure from [Cav09]).

#### 1.2.2 The phase diagram of glasses

As explained in [MP09, PZ10], the phase diagram of a glass has many important domains separated by precise points, which will interest us all along the next sections. This study can be done by decreasing the temperature or increasing the pressure or the density (or the packing fraction). For a best view of this, the figure 4 is drawn as the inverse of the pressure versus the packing fraction but for a better comprehension, the explanation will be done by decreasing the temperature because many phenomena are better understood at fixed temperature than at fixed density.

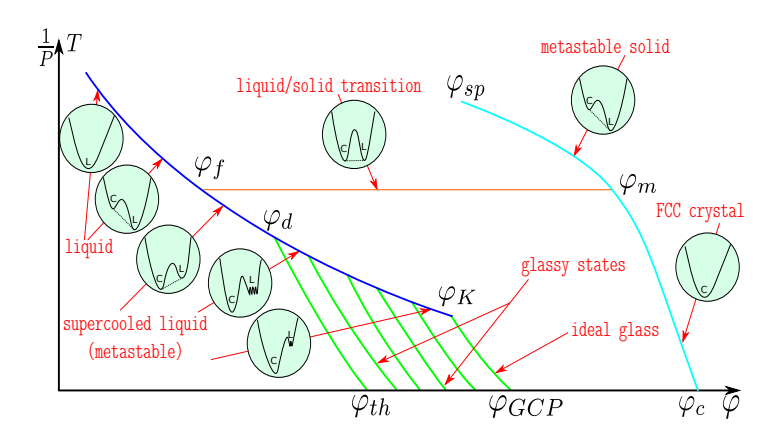


FIGURE 4 – Phase diagram of glasses in the representation of the inverse of the pressure (or the temperature) versus the packing fraction. In the little circles, the free energy behaviour is represented with L corresponding to the liquid state and C to the crystal state.

We suppose that we start from a temperature higher than the spinodal temperature  $T_{sp}$  of the solid, to be in a liquid configuration. While  $T > T_{sp}$ , the free energy has only one minimum and corresponds to the liquid state. Between  $T_{sp}$  and  $T_f$ , the freezing temperature, the free energy looses that convexity and a second minimum appears, which corresponds to the crystal state, with a bigger free energy than the first minimum, which corresponds to the liquid state.

When  $T = T_f$ , the two minima of the free energy have the same value and thus a first order phase transition happens. If the quench of temperature is fast enough, the liquid does not crystallize at  $T = T_f$  (and does not follow the Maxwell construction of free energy) and so becomes a supercooled liquid which follows the prolongation of the free energy expression. If the spinodal temperature of the liquid is small enough, the supercooled liquid will not crystallize before the glass transition.

Between  $T_f$  and  $T_d$ , the dynamical temperature, the free energy has two minima with a global one, which corresponds to the crystal state.

At  $T=T_d$ , the dynamical transition happens, the liquid minimum divides into an exponentially large number of minima, each one corresponding to a glassy state. The configurational entropy, or complexity, is defined as the logarithm of this number of minima, which corresponds to the number of glassy states. At this step, the dynamical correlation diverges and the first glassy state can appear. If the supercooled liquid transforms into a glass and follows the glass line, the pressure diverges at the jammed state  $\varphi_{th}$  corresponding to  $T_d$ , called the threshold packing fraction.

If the cooling is slow enough, the glass transition can happen between  $T_d$  and  $T_K$ , the Kauzmann temperature. The value of the free energy is still given by the prolongation of the liquid one. The time to go from a minimum to another is large. The appearence of metastable glassy states in this domains can associate to the supercooled liquid a jammed state  $\varphi_j(T)$  obtained by cooling the configuration fast enough. The complexity decreases all along this interval.

At  $T = T_K$ , the complexity cancels and the liquid disappers for lower temperature. At this point, the thermodynamical transition happens and the capacity  $C_v$  has a jump.

For  $T < T_K$ , the glass is unique and goes to the jammed state  $\varphi_{GCP} < \varphi_{crystal}$ , call the close packing fraction, at zero temperature. At dimension 3,  $\varphi_{GCP} \sim 0.64$  and  $\varphi_{crystal} \sim 0.74$ . This corresponds to the ideal transition, which is unobservable in practice due to the speed of the quench which is not slow enough.

#### 1.2.3 The replica method

To compute the entropy of the glass, as done in [MP09, PZ10], we introduce m copies ("replicas") of the original system with an attractive potential  $\epsilon \to 0$  between them, to study the auto-induced disorder coming from the many equilibrium configurations. Historically, the replicas were introduced to calculate the  $\log Z$  as  $\lim_{m\to 0} \frac{\partial}{\partial m} Z^m$  in the spin glass problem.

The partition function is written as  $Z = e^{NS(\varphi)} = \sum_{\alpha} e^{Ns_{\alpha}}$  with the sum over the state of vibrational entropy  $s_{\alpha}$ . The configurational entropy or complexity of internal entropy s is defined as

$$\Sigma(s,\varphi) = \frac{1}{N} \log \mathcal{N}(s) \tag{1.2.5}$$

with  $\mathcal{N}(s)$  the number of states of entropy s. The partition function becomes  $Z = \int ds e^{N(s+\Sigma)} \sim e^{N(s^*+\Sigma(s^*,\varphi))}$  with  $s^*$  the place of the maximum of  $S(\varphi)$ .

We define thus the replicated partition function as  $Z_m = \sum_{\alpha} e^{Nms_{\alpha}} \sim e^{NS(m,\varphi,s^*)}$  with  $S(m,\varphi,s) = ms + \Sigma(s,\varphi)$ with  $s^*(m,\varphi) = \frac{\partial S}{\partial m}(m,\varphi,s)$ . From this we define a Legendre transformation to have only  $(m,\varphi)$  as parameter. The complexity becomes

$$\Sigma(m,\varphi) = \Sigma(s^*(m,\varphi),\varphi) = S(m,\varphi) - ms^*(m,\varphi)$$

$$s^*(m,\varphi) = \frac{\partial S}{\partial m}(m,\varphi)$$
(1.2.6)

From this we get the phase diagram  $(m, \varphi)$ , the mirror of the  $(p,\varphi)$  diagram, reproduced in figure 5. For each density  $\varphi > \varphi_{TAP}$ , we can define a point  $m_s(\varphi)$  as the solution of  $\Sigma(m,\varphi) = 0$ . On this line, we see that  $S(m,\varphi) = ms_{max}$ , then

$$S_{glass}(m,\varphi) = s_{max}(\varphi) = \frac{S(m_s(\varphi),\varphi)}{m_s(\varphi)}$$
(1.2.7)

and thus define the ideal glass line. For each density  $\varphi > \varphi_{TAP}$ , we can also define a point  $m_d(\varphi)$  which corresponds to the minimum value  $s_{min}$ , below which there are no states. We call  $m_d(\varphi)$  the clustering line because above this line the space of configuration is disconnected in many clusters corresponding to the glassy states. All these states are found between this two lines. The jammed states are obtained for m=0 and the equilibrium states for m=1.

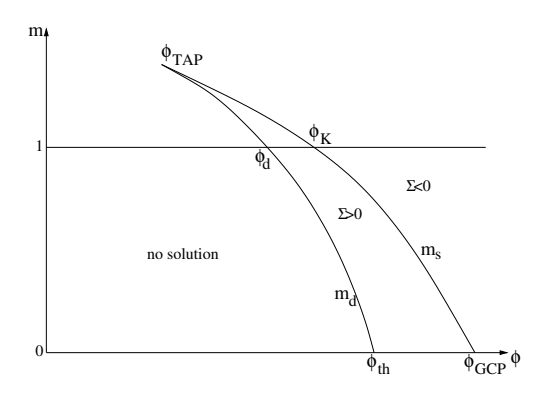


FIGURE 5 – Phase diagram of glasses in the  $(m, \varphi)$  space with the clustering and ideal glass lines (Figure from [PZ10]).

The m replicas are represented by molecules, described by  $\bar{x} = \{x_1, ..., x_m\}$  where  $x_i$  is a d-dimension vector. The replicated liquid is characterized by the density  $\rho_a(x) = \langle \delta^{(d)}(x - x_a) \rangle$  of each replica and by the correlation function  $\rho_{ab}(x,y) = \langle \delta^{(d)}(x-x_a)\delta^{(d)}(y-x_b) \rangle$ . The replicated pair correlation is  $g_{ab} = \frac{\rho_{ab}(x,y)}{\rho_a(x)\rho_b(y)}$ . If there is a symmetry between the replicas,  $\rho_a(x) = \rho$ , the intrareplica correlation becomes  $g(x-y) = g_{aa}(x,y) = \rho^{-2}\rho_{aa}(x,y)$  and the interreplica correlation becomes  $\tilde{g}(x-y) = g_{a\neq b}(x,y) = \rho^{-2}\rho_{a\neq b}(x,y)$ . Due to the translation invariance, the averages over states become,  $\overline{\rho_a(x)} = \rho(x)$ ,  $g(x-y) = \rho^{-2}\overline{\rho_{aa}(x,y)}$  and  $\tilde{g}(x-y) = \rho^{-2}\overline{\rho_{a}(x)\rho_{a}(x)}$ . If there is no interaction between replicas,  $\tilde{q}(x-y)=1$ .

The replicated Hyper Netted Chain equations are the same than the liquid one for the intrareplica correlation g(r)and are replaced for the interreplica correlation  $\tilde{g}(r)$  by

$$\tilde{c}(r) = \tilde{h}(r) - \log[1 + \tilde{h}(r)] \text{ and } \hat{\tilde{c}}(k) = \frac{1 - \rho \hat{c}(k)}{1 + \rho[\hat{h}(k) - \hat{\tilde{h}}(k)]} \hat{\tilde{h}}(k)$$
 (1.2.8)

where the  $\hat{f}$  functions are the interreplica function corresponding to the intraregular function f and where the  $\hat{f}(k)$ functions correspond to the Fourier transform of f(r).

#### 2 Derivation of equations for the entropy and the phase diagram

In this section, we will derive the expression of the entropy for the replicated system and from it, deduce the equations for the complexity and for all quantities of the phase diagram:  $\varphi_d$ ,  $\varphi_K$ ,  $\varphi_{th}$  and  $\varphi_{GCP}$ .

#### 2.1The replicated entropy

We want to solve this problem introducing m replicas arranged into point-like molecules, if the cage radius  $A \equiv$ 

 $\frac{1}{2dN}\langle (x_a-x_b)^2\rangle$  is zero, described by  $\bar{x}=\{x_1,...,x_m\}$  where  $x_i$  is a d-dimension vector. We start from the expression of the entropy  $S[\rho,g]$  of a molecular liquid in term of single-particle density  $\rho(\bar{x})$ , the correlation of two molecules  $g(\bar{x}, \bar{y})$  and the interaction potential between two molecules  $v(\bar{x}, \bar{y}) = \sum_{\alpha=1}^{m} v(|x^{\alpha} - y^{\alpha}|)$ . We neglect the 2PI diagrams and therefore consider the so-called HNC approximation. Using the expression of the entropy of the liquid (1.1.25) and the replica method, we have

$$S[\rho,g] = \frac{1}{N} \int d\bar{x} \rho(\bar{x}) [\log \rho(\bar{x}) - 1] - \frac{1}{2N} \int d\bar{x} d\bar{y} \rho(\bar{x}) \rho(\bar{y}) \{g(\bar{x},\bar{y})[\log g(\bar{x},\bar{y}) + \beta v(\bar{x},\bar{y}) - 1] + 1\} + \frac{1}{2N} \sum_{n \geq 3} \frac{(-1)^n}{n} Tr_x [\rho h]^n \quad (2.1.1)$$

where  $h(\bar{x}, \bar{y}) = g(\bar{x}, \bar{y}) - 1$  and  $Tr_x[\rho h]^n = \int d\bar{x}_1...d\bar{x}_n \rho(\bar{x}_1)h(\bar{x}_1, \bar{x}_2)\rho(\bar{x}_2)h(\bar{x}_2, \bar{x}_3)...\rho(\bar{x}_n)h(\bar{x}_n, \bar{x}_1)$ .

This expression is variational and should be minimized with respect to  $\rho$  and g. We assume, for the single-particle density, the Gaussian form (2.1.2) and, for the pair correlation factorized form (2.1.3) where  $G(\vec{r})$  is an unknown

function and the contribution of the term in parenthesis is small if A is small, because the Gaussian form forces  $x_a$  to be close to X. We define also  $Q(\vec{r})$  as (2.1.4) assumed to be small, H = G - 1 and C from (2.1.5).

$$\rho(\bar{x}) = \rho \int d^d X \prod_{\alpha=1}^m \gamma_A(x_\alpha - X) = \rho \frac{m^{-d/2}}{(2\pi A)^{(m-1)d/2}} \exp\left[ -\frac{1}{2mA} \sum_{\alpha < \beta} (x^\alpha - x^\beta)^2 \right], \quad \gamma_A(u) = \frac{e^{-\frac{u^2}{2A}}}{(2\pi A)^{d/2}}$$
(2.1.2)

$$g(\bar{x}, \bar{y}) = \rho^{-2} \rho(\bar{x}) \rho(\bar{y}) \prod_{\alpha=1}^{m} e^{-\beta v_r(x^{\alpha} - y^{\alpha})} = G(X - Y) + \left[ \prod_{\alpha=1}^{m} G(|x^{\alpha} - y^{\alpha}|)^{1/m} - G(X - Y) \right]$$
(2.1.3)

$$Q(\vec{r}) = \left( \int d^d \vec{u} \gamma_{2A}(\vec{u}) G(\vec{r} - \vec{u})^{1/m} \right)^m - G(\vec{r})$$
 (2.1.4)

$$\rho \int d^{d}\vec{u}H(\vec{r} - \vec{u})C(\vec{u}) = H(\vec{r}) - C(\vec{r})$$
(2.1.5)

With these approximations, we can expand at the first order in Q

$$\frac{1}{N} \int d\bar{x} \rho(\bar{x}) [\log \rho(\bar{x}) - 1] = 1 - \log \rho + \frac{d}{2} (m - 1) \log(2\pi A) + \frac{d}{2} (m - 1 + \log m) 
\frac{1}{N} \int d\bar{x} d\bar{y} \rho(\bar{x}) \rho(\bar{y}) g(\bar{x}, \bar{y}) = \rho \int d^d \vec{r} [G(\vec{r}) + Q(\vec{r})] 
\frac{1}{2N} \int d\bar{x} d\bar{y} \rho(\bar{x}) \rho(\bar{y}) g(\bar{x}, \bar{y}) [\log g(\bar{x}, \bar{y}) + \beta v(\bar{x}, \bar{y})] = \rho \int d^d \vec{r} [G(\vec{r}) + Q(\vec{r})] \cdot [\log G(\vec{r}) + \beta m v(\vec{r})] 
\frac{1}{N} \sum_{n \ge 3} \frac{(-1)^n}{n} Tr_x [\rho h]^n = \frac{1}{N} \sum_{n \ge 3} \frac{(-1)^n}{n} Tr_x H^n - \rho \int d^d \vec{r} Q(\vec{r}) [H(\vec{r}) - C(\vec{r})]$$
(2.1.6)

Collecting all the terms, using the HNC equation (1.1.23, 2.1.7) and the relation (2.1.8), we obtain a straightforward optimization over G(r)

$$\log G(\vec{r}) + \beta m v(\vec{r}) - H(\vec{r}) + C(\vec{r}) = 0$$
(2.1.7)

$$\frac{1}{N} \sum_{n \geq 3} \frac{(-1)^n}{n} Tr_x H^n = \frac{1}{\rho} \int \frac{d^d \vec{k}}{(2\pi)^d} [\log(1 + \rho \hat{H}(\vec{k})) - \rho \hat{H}(\vec{k}) + \frac{1}{2} \rho^2 \hat{H}(\vec{k})^2], \quad \hat{H}(\vec{k}) = \int d^d \vec{r} e^{i\vec{k} \cdot \vec{r}} H(\vec{r})$$
(2.1.8)

In fact, at the lowest order, the correction  $G_m(A, \varphi)$  of  $S[\rho, g] = S(m, A; T, \varphi)$  as defined in (2.1.10) is not needed and therefore we simply obtain

$$G(r) = g_{liq}(r; \frac{T}{m}, \varphi), \quad \hat{H}(k) = \hat{h}_{liq}(r; \frac{T}{m}, \varphi)$$
(2.1.9)

where  $g_{liq}$  is the correlation function of the normal liquid with potential v at temperature  $T = 1/\beta$  and packing fraction  $\varphi$ .

The result of this procedure for the replicated entropy is the following, where  $I_n(x)$  is the modified Bessel function.

$$S(m, A; T, \varphi) = S_{liq}^{HNC}(\varphi) + S_{harm}(m, A) + 2^{d-1}\varphi G_m(A, \varphi)$$

$$S_{liq}^{HNC}(\varphi) = 1 - \log \rho - 2^{d-1}\varphi d \int_0^\infty dr r^{d-1} \left\{ g_{liq}(r; \frac{T}{m}, \varphi) \left[ \log g_{liq}(r; \frac{T}{m}, \varphi) + \beta m v(r) - 1 \right] + 1 \right\}$$

$$+ \frac{2^{d-1}\varphi d}{(2\pi)^d \rho^2} \int_0^\infty dk k^{d-1} \left[ \log(1 + \rho \hat{h}_{liq}(k; \frac{T}{m}, \varphi)) - \rho \hat{h}_{liq}(k; \frac{T}{m}, \varphi) + \frac{1}{2} (\rho \hat{h}_{liq}(k; \frac{T}{m}, \varphi))^2 \right]$$

$$S_{harm}(m, A) = \frac{d}{2}(m - 1) \log(2\pi A) + \frac{d}{2}(m - 1 + \log m)$$

$$G(m, A, \varphi) = d \int_0^\infty dr r^{d-1} Q(r) = d \int_0^\infty dr r^{d-1} \left[ q_{A,m}(r, \varphi)^m - g_{liq}(r; \frac{T}{m}, \varphi) \right]$$

$$q_{A,m}(r, \varphi) = \int d\vec{u} \gamma_A(\vec{r} - \vec{u}) g_{liq}(\vec{u}; \frac{T}{m}, \varphi)^{\frac{1}{m}} = \int_0^\infty du g_{liq}(u; \frac{T}{m}, \varphi)^{\frac{1}{m}} \left( \frac{u}{r} \right)^{\frac{d-1}{2}} \frac{e^{-\frac{(r-u)^2}{4A}}}{\sqrt{4\pi A}} \left[ e^{-\frac{ru}{2A}} \sqrt{\pi \frac{ru}{A}} I_{\frac{d-2}{2}} \left( \frac{ru}{2A} \right) \right]$$

$$(2.1.10)$$

From now on, we will consider hard spheres and thus T=0 and  $\beta mv(r)g_{liq}(r;\frac{T}{m},\varphi)=0$ .

#### 2.2 The equation for A

From the equations (2.1.10) we can derive the equation for A from the condition  $\frac{\partial S}{\partial A} = 0$ , which reads

$$1 = \frac{2^{d} \varphi}{d} \frac{A}{1 - m} \frac{\partial G_{m}}{\partial A} (A, \varphi) = \frac{2^{d} \varphi}{d} F_{m}(A, \varphi)$$

$$F_{m}(A, \varphi) = \frac{dAm}{1 - m} \int_{0}^{\infty} dr r^{d-1} \frac{\partial q_{A,m}}{\partial A} (r, \varphi) q_{A,m}(r, \varphi)^{m-1}$$
(2.2.1)

For a fixed m,  $F_m(A, \varphi)$  presents a maximum which determines the clustering line : if the equations (2.2.1) do not have any solution, the packing fraction  $\varphi$  corresponds to a liquid state, otherwise it corresponds to a glassy state.

Thus, the equation for the clustering line is

$$1 = \frac{2^d \varphi}{d} \max_{A} F_m(A, \varphi)$$
 (2.2.2)

# 2.3 The complexity

From the equations (1.2.6) and (2.1.10) we can derive the equation for the complexity as follows

$$\Sigma_{m}(A,\varphi) = S(m,A,\varphi) - m\frac{\partial S}{\partial m}(m,A,\varphi) = S_{liq}(\varphi) - \frac{d}{2}\log(2\pi A) + \frac{d}{2}(\log m - 2) + 2^{d-1}\varphi H_{m}(A,\varphi)$$

$$H_{m}(A,\varphi) = d\int_{0}^{\infty} dr r^{d-1}[q_{A,m}(r,\varphi)^{m} - g_{liq}(r,\varphi) - m^{2}\frac{\partial q_{A,m}}{\partial m}(r,\varphi)q_{A,m}^{m-1}(r,\varphi) - mq_{A,m}(r,\varphi)^{m}\log q_{A,m}(r,\varphi)]$$
(2.3.1)

The complexity exists only if A is a solution of (2.2.1). A glassy state exists only if the complexity is positive. We define the ideal glass line, the highest density at which a glass can be formed at a fixed pression, as the solution of  $\Sigma_m(A,\varphi)=0$ .

Thus, the equation for the ideal glass line is

$$\Sigma_m(A,\varphi) = S_{liq}(\varphi) - \frac{d}{2}\log(2\pi A) + \frac{d}{2}\log m - d + 2^{d-1}\varphi H_m(A,\varphi) = 0$$
(2.3.2)

# 2.4 The equilibrium equations $(\varphi_d, \varphi_K)$

The equilibrium line is defined by m=1, as seen in Figure 5. The packing fraction corresponding to the clustering line is the dynamical packing fraction  $\varphi_d$  and the one corresponding to the ideal glass line is the Kauzmann packing fraction  $\varphi_K$ .

From the equations (2.2.1) and (2.2.2) we get the equations for  $\varphi_d$ 

$$1 = \frac{2^{d} \varphi}{d} \max_{A} F_{1}(A, \varphi), \quad F_{1}(A, \varphi) = -dA \int_{0}^{\infty} dr r^{d-1} \frac{\partial q_{A}}{\partial A}(r, \varphi) \log q_{A}(r, \varphi)$$
(2.4.1)

From the equations (2.2.1) and (2.3.2) we get the equations for  $\varphi_K$ , using the fact that  $\int d\vec{r} q_{A,1}(\vec{r},\varphi) = \int d\vec{r} g_{liq}(\vec{r},\varphi)$ 

$$\Sigma_{eq}(A,\varphi) = \Sigma_{1}(A,\varphi) = S_{liq}(\varphi) - \frac{d}{2}\log(2\pi A) - d - 2^{d-1}d\varphi \int_{0}^{\infty} dr r^{d-1} [q_{A}(r,\varphi)\log q_{A}(r,\varphi) + \widetilde{q_{A}}(r,\varphi)] = 0$$

$$1 = -dA \frac{2^{d}\varphi}{d} \int_{0}^{\infty} dr r^{d-1} \frac{\partial q_{A}}{\partial A}(r,\varphi)\log q_{A}(r,\varphi)$$
(2.4.2)

where the expression of  $q_A(r,\varphi)$ ,  $\frac{\partial q_A}{\partial A}(r,\varphi)$  and  $\widetilde{q_A}(r,\varphi)$  are

$$q_{A}(r,\varphi) = \int_{0}^{\infty} du g_{liq}(u,\varphi) \left(\frac{u}{r}\right)^{\frac{d-1}{2}} \frac{e^{-\frac{(r-u)^{2}}{4A}}}{\sqrt{4\pi A}} \left[e^{-\frac{ru}{2A}} \sqrt{\pi \frac{ru}{A}} I_{\frac{d-2}{2}} \left(\frac{ru}{2A}\right)\right]$$

$$\frac{\partial q_{A}}{\partial A}(r,\varphi) = \int_{0}^{\infty} du g_{liq}(u,\varphi) \left(\frac{u}{r}\right)^{\frac{d-1}{2}} \frac{e^{-\frac{(r-u)^{2}}{4A}}}{\sqrt{4\pi A}} \frac{1}{4A^{2}} \left\{e^{-\frac{ru}{2A}} \sqrt{\pi \frac{ru}{A}} \left[\left(r^{2} + u^{2} - 2dA\right) I_{\frac{d-2}{2}} \left(\frac{ru}{2A}\right) - 2ru I_{\frac{d}{2}} \left(\frac{ru}{2A}\right)\right]\right\}$$

$$\widetilde{q_{A}}(r,\varphi) = -\int_{0}^{\infty} du g_{liq}(u,\varphi) \log g_{liq}(u,\varphi) \left(\frac{u}{r}\right)^{\frac{d-1}{2}} \frac{e^{-\frac{(r-u)^{2}}{4A}}}{\sqrt{4\pi A}} \left[e^{-\frac{ru}{2A}} \sqrt{\pi \frac{ru}{A}} I_{\frac{d-2}{2}} \left(\frac{ru}{2A}\right)\right]$$

$$(2.4.3)$$

# 2.5 The jamming equations $(\varphi_{th}, \varphi_{GCP})$

The jamming line is defined by m=0. The packing fraction corresponding to the clustering line is the threshold packing fraction  $\varphi_{th}$  and the one corresponding to the ideal glass line is the Glass Close Packing fraction  $\varphi_{GCP}$ . When m vanishes, A behaves as  $A=m\alpha$ .

Using  $\lim_{z\to\infty} \sqrt{2\pi z} e^z I_n(z) = 1$  and  $g_{liq}(r,\varphi) = 0$  for  $r \in [0,1[$ , we get

$$\lim_{m \to 0} q_{A,m}(r,\varphi) = \lim_{m \to 0} \int_{1}^{\infty} du g_{liq}(u,\varphi)^{\frac{1}{m}} \left(\frac{u}{r}\right)^{\frac{d-1}{2}} \frac{e^{-\frac{(r-u)^{2}}{4m\alpha}}}{\sqrt{4\pi m\alpha}} = \begin{cases} \lim_{m \to 0} g_{liq}(r,\varphi)^{\frac{1}{m}} & r > 1\\ \lim_{m \to 0} g_{liq}(1,\varphi)^{\frac{1}{m}} \left(\frac{1}{r}\right)^{\frac{d-1}{2}} \frac{e^{-\frac{(r-1)^{2}}{4m\alpha}}}{\sqrt{4\pi m\alpha}} & r < 1 \end{cases}$$
(2.5.1)

$$-\lim_{m\to 0} m^2 \frac{\partial q_{A,m}}{\partial m}(r,\varphi) = \begin{cases} \lim_{m\to 0} g_{liq}(r,\varphi)^{\frac{1}{m}} \log g_{liq}(r,\varphi) & r > 1\\ \lim_{m\to 0} g_{liq}(1,\varphi)^{\frac{1}{m}} \log g_{liq}(1,\varphi) \left(\frac{1}{r}\right)^{\frac{d-1}{2}} \frac{e^{-\frac{(r-1)^2}{4m\alpha}}}{\sqrt{4\pi m\alpha}} & r < 1 \end{cases}$$
(2.5.2)

$$\lim_{m \to 0} q_{A,m}(r,\varphi)^m = \begin{cases} g_{liq}(r,\varphi) & r > 1\\ g_{liq}(1,\varphi)e^{-\frac{(r-1)^2}{4\alpha}} & r < 1 \end{cases}$$
 (2.5.3)

We obtain then the equation for  $F_0(\alpha, \varphi)$  from (2.2.1),  $H_0(\alpha, \varphi)$  and  $\Sigma_j(\alpha, \varphi)$  from (2.3.1) using the fact that  $F_0(\alpha, \varphi) \cdot \frac{2^d \varphi}{d} = 1$ ,

$$F_{0}(\alpha,\varphi) = \lim_{m \to 0, A = \alpha m} \frac{dA}{1 - m} \frac{\partial}{\partial A} \int_{0}^{\infty} dr r^{d-1} [q_{A,m}(r,\varphi)^{m} - g_{liq}(r,\varphi)] = d\alpha \frac{\partial}{\partial \alpha} \int_{0}^{1} dr r^{d-1} g_{liq}(1,\varphi) e^{-\frac{(r-1)^{2}}{4\alpha}}$$

$$= \frac{d}{4\alpha} g_{liq}(1,\varphi) \int_{0}^{1} dr r^{d-1} (r-1)^{2} e^{-\frac{(r-1)^{2}}{4\alpha}}$$

$$(2.5.4)$$

$$H_{0}(\alpha,\varphi) = \lim_{m \to 0, A = \alpha m} d \int_{0}^{\infty} dr r^{d-1} \left\{ q_{A,m}(r,\varphi)^{m} \left[ 1 - \frac{m^{2}}{q_{A,m}(r,\varphi)} \frac{\partial q_{A,m}}{\partial m}(r,\varphi) - \log q_{A,m}(r,\varphi)^{m} \right] - g_{liq}(r,\varphi) \right\}$$

$$= dg_{liq}(1,\varphi) \int_{0}^{1} dr r^{d-1} e^{-\frac{(r-1)^{2}}{4\alpha}} \left[ 1 + \frac{(r-1)^{2}}{4\alpha} \right] = dg_{liq}(1,\varphi) \int_{0}^{1} dr r^{d-1} e^{-\frac{(r-1)^{2}}{4\alpha}} + \frac{d}{2^{d}\varphi}$$

$$(2.5.5)$$

$$\Sigma_{j}(\alpha,\varphi) - S_{liq}(\varphi) = -\frac{d}{2}\log(2\pi\alpha) - d + 2^{d-1}\varphi H_{0}(\alpha,\varphi) = -\frac{d}{2}[\log(2\pi\alpha) + 1] + 2^{d-1}d\varphi g_{liq}(1,\varphi) \int_{0}^{1} dr r^{d-1} e^{-\frac{(r-1)^{2}}{4\alpha}}$$
(2.5.6)

From the equations (2.2.1) and (2.2.2) we get then the equation for  $\varphi_{th}$ 

$$1 = \frac{2^{d}\varphi}{d} \max_{\alpha} F_{0}(\alpha, \varphi), \quad F_{0}(\alpha, \varphi) = \frac{d}{4\alpha} g_{liq}(1, \varphi) \int_{0}^{1} dr r^{d-1} (r-1)^{2} e^{-\frac{(r-1)^{2}}{4\alpha}}$$
(2.5.7)

From the equations (2.2.1) and (2.3.2) we get then the equation for  $\varphi_{GCP}$ 

$$\Sigma_{j}(\alpha,\varphi) = \lim_{m \to 0} \Sigma_{m}(m\alpha,\varphi) = S_{liq}(\varphi) - \frac{d}{2}[\log(2\pi\alpha) + 1] + 2^{d-1}d\varphi g_{liq}(1,\varphi) \int_{0}^{1} dr r^{d-1} e^{-\frac{(r-1)^{2}}{4\alpha}} = 0$$

$$1 = \frac{2^{d}\varphi}{d} \frac{d}{4\alpha} g_{liq}(1,\varphi) \int_{0}^{1} dr r^{d-1} (r-1)^{2} e^{-\frac{(r-1)^{2}}{4\alpha}}$$
(2.5.8)

# 3 Dimensional behaviour of the phase diagram

In this section, we will start to verify the consistency of the derived equations with previous approaches as the high-dimensional bahaviour and the small cage expansion done in [PZ10]. We will finish by showing the numerical solution of these derived equations to get the different densities  $\varphi_d$ ,  $\varphi_K$ ,  $\varphi_{th}$  and  $\varphi_{GCP}$ .

# 3.1 Asymptotic behaviour

Here, we will derive the asymptotic behaviour of different densities. Some parts of this calculation and the next results can be found in [PZ10].

### **3.1.1** Derivation of $q_A(r)$

When  $d \to \infty$ , A vanishes as  $A = \frac{\hat{A}}{d^2}$  form [PZ10]. Thus, in  $q_{A,m}$ , we need to evaluate the behaviour of  $I_{\frac{d-2}{2}}(d^2z)$  with  $z = \frac{ru}{2\hat{A}}$  a fixed parameter.

$$I_n(x) = \frac{1}{2\pi i} \int_0^\infty dt t^{-(n+1)} e^{\frac{x}{2}(t+\frac{1}{t})} \Rightarrow I_{\frac{d-2}{2}}(d^2z) = \frac{1}{2\pi i} \int_0^\infty dt t^{-\frac{d}{2}} e^{\frac{d^2z}{2}(t+\frac{1}{t})}$$
(3.1.1)

For  $d \to \infty$ , we can use the saddle-point method such that

$$I_{\frac{d-2}{2}}(d^2z) = \frac{1}{2\pi i} \int_{-\infty}^{\infty} dt e^{-df(z,t)} = \frac{1}{\sqrt{-2\pi z f''(z,t_0)}} e^{-df(z,t_0)}, \quad f(z,t) = \frac{1}{2} \left[ \log t - dz \left( t + \frac{1}{t} \right) \right] \text{ and } f'(z,t_0) = 0 \quad (3.1.2)$$

In this case, we get at the first orders in 1/d,

$$f'(z,t_0) = \frac{1}{2} \left[ \frac{1}{t_0} - dz \left( 1 - \frac{1}{t_0^2} \right) \right] = 0 \Rightarrow t_0 = \frac{1 + \sqrt{1 + 4d^2z^2}}{2dz} \sim 1 + \frac{1}{2dz} + \frac{1}{8d^2z^2}$$

$$f(z,t_0) = \frac{1}{2} \left[ \log t_0 - dz \left( t_0 + \frac{1}{t_0} \right) \right] \sim -dz + \frac{1}{8dz}$$

$$f''(z,t_0) = -\frac{1}{2} \left( \frac{1}{t_0^2} - \frac{2dz}{t_0^3} \right) \sim -dz + 1 - \frac{5}{8dz}$$

$$(3.1.3)$$

Thus, the high-dimension behaviour of the modified Bessel function is

$$I_{\frac{d-2}{2}}(d^2z) = \frac{1}{\sqrt{2\pi d^2z}}e^{d^2z - \frac{1}{8z}}$$
(3.1.4)

From this computation, we can now evaluate  $q_{A,m}$  for  $d \to \infty$ , putting  $g_{liq}(r,\varphi) = \theta(r-1)$  (thus  $q_{A,m}$  does not depend on m anymore) and  $A = \frac{\hat{A}}{d^2}$ 

$$q_A(r) = d \int_1^\infty du \left(\frac{u}{r}\right)^{\frac{d-1}{2}} \frac{e^{-\frac{d^2(r-u)^2}{4\hat{A}}}}{\sqrt{4\pi\hat{A}}} e^{-\frac{\hat{A}}{4ru}}$$
(3.1.5)

Taking the change of variables (used all along this section),  $t = \frac{d(r-1)}{\sqrt{4\hat{A}}} = \frac{y}{\sqrt{4\hat{A}}}$  and  $s = \frac{d(u-1)}{\sqrt{4\hat{A}}}$ , we get

$$q_{A}(t) = \int_{0}^{\infty} \frac{ds}{\sqrt{\pi}} e^{-(s-t-\frac{\sqrt{\hat{A}}}{2})^{2}} = \int_{t+\frac{\sqrt{\hat{A}}}{2}}^{\infty} \frac{ds}{\sqrt{\pi}} e^{-s^{2}} = \Theta\left(t + \frac{\sqrt{\hat{A}}}{2}\right), \quad q_{A}(y) = \Theta\left(\frac{y + \hat{A}}{\sqrt{4\hat{A}}}\right)$$
(3.1.6)

with  $\Theta(t) = \frac{1}{2} (1 + \operatorname{erf}(t))$ 

# **3.1.2** Derivation of $S_{liq}(\varphi)$

From the definition of the entropy of the liquid (1.1.29), we get for  $g_{liq}(1,\varphi)=1$ 

$$S_{liq}(\varphi) = 1 - \log \rho - 2^{d-1} \int_0^{\varphi} d\varphi' g_{liq}(1, \varphi') = 1 - \log \rho - 2^{d-1} \varphi$$
(3.1.7)

Taking  $\hat{\varphi} = \frac{2^d}{d} \varphi$  and  $\rho = \frac{2^d \varphi}{\pi^{d/2}} \Gamma(\frac{d}{2} + 1)$ ,

$$S_{liq}(\varphi) = 1 - \log \left[ \frac{\hat{\varphi}d}{\pi^{d/2}} \Gamma\left(\frac{d}{2} + 1\right) \right] - \frac{d}{2}\hat{\varphi}$$
(3.1.8)

From the Stirling formula, we get finally

$$S_{liq}(\varphi) = 1 - \log(\sqrt{\pi d^3}\hat{\varphi}) + \frac{d}{2} \left[ \log\left(\frac{2\pi}{d}\right) + 1 - \hat{\varphi} \right]$$
(3.1.9)

#### 3.1.3 Derivation of densities

#### Dynamical and threshold packing fractions

Using the expression of  $q_A$  and  $g_{liq}(1,\varphi) = 1$ , we get the expressions of  $F_1$  from (2.4.1) and  $F_0$  from (2.5.7)

$$F_{1}(A,\varphi) = -dA \int_{0}^{\infty} dr r^{d-1} \frac{\partial q_{A}}{\partial A}(r,\varphi) \log q_{A}(r,\varphi) = -\hat{A} \int_{-\infty}^{\infty} dy e^{y} \frac{\partial}{\partial \hat{A}} \Theta\left(\frac{y+\hat{A}}{\sqrt{4\hat{A}}}\right) \log \Theta\left(\frac{y+\hat{A}}{\sqrt{4\hat{A}}}\right)$$

$$= \frac{1}{4\sqrt{\pi\hat{A}}} \int_{-\infty}^{\infty} dy (y-\hat{A}) e^{-\frac{(y-\hat{A})^{2}}{4\hat{A}}} \log \Theta\left(\frac{y+\hat{A}}{\sqrt{4\hat{A}}}\right) = \sqrt{\frac{\hat{A}}{\pi}} \int_{-\infty}^{\infty} dt t e^{-t^{2}} \log \Theta\left(t+\sqrt{\hat{A}}\right)$$

$$F_{0}(\alpha,\varphi) = \frac{d}{4\alpha} g_{liq}(1,\varphi) \int_{0}^{1} dr r^{d-1} (r-1)^{2} e^{-\frac{(r-1)^{2}}{4\alpha}} = \frac{1}{4\hat{\alpha}} \int_{0}^{\infty} dy y^{2} e^{-y-\frac{y^{2}}{4\hat{\alpha}}} = -\hat{\alpha} + (1+2\hat{\alpha})\sqrt{\hat{\alpha}} e^{\hat{\alpha}} \int_{\sqrt{\hat{\alpha}}}^{\infty} dt e^{-t^{2}}$$

$$(3.1.10)$$

From this, we get the high-dimensional behaviour of  $\varphi_d$  and  $\varphi_{th}$ 

$$\varphi_d = \frac{d}{2^d} \hat{\varphi}_d, \quad \lim_{d \to \infty} \hat{\varphi}_d^{-1} = \max_{\hat{A}} \sqrt{\frac{\hat{A}}{\pi}} \int_{-\infty}^{\infty} dt t e^{-t^2} \log \Theta \left( t + \sqrt{\hat{A}} \right)$$
(3.1.11)

$$\varphi_{th} = \frac{d}{2^d} \hat{\varphi}_{th}, \quad \lim_{d \to \infty} \hat{\varphi}_{th}^{-1} = \max_{\hat{\alpha}} \left[ -\hat{\alpha} + (1 + 2\hat{\alpha})\sqrt{\pi\hat{\alpha}}e^{\hat{\alpha}}\Theta\left(-\sqrt{\hat{\alpha}}\right) \right]$$
(3.1.12)

With a numerical analysis, we get

$$\lim_{d \to \infty} \hat{\varphi}_d = 4.8067787, \quad \lim_{d \to \infty} \hat{A}_d = 0.5766799$$
(3.1.13)

$$\lim_{d \to \infty} \hat{\varphi}_{th} = 6.2581221, \quad \lim_{d \to \infty} \hat{\alpha}_{th} = 0.3024338$$
 (3.1.14)

#### Kauzmann and close packing fractions

Using the expression of  $q_A$  and  $S_{liq}$ , we can derive the expression of  $\Sigma_{eq}$  from (2.4.2),

$$\Sigma_{eq}(A,\varphi) = S_{liq}(\varphi) - \frac{d}{2}\log(2\pi A) - d - 2^{d-1}d\varphi \int_{0}^{\infty} dr r^{d-1} \left[ q_{A}(r,\varphi) \log q_{A}(r,\varphi) + g_{liq}(r,\varphi) \log g_{liq}(r,\varphi) \right]$$

$$= 1 - \log(\sqrt{\pi d^{3}}\hat{\varphi}) + \frac{d}{2} \left\{ \log \frac{d}{\hat{A}} - 1 - \hat{\varphi} \left[ 1 + \int_{-\infty}^{\infty} dy e^{y} \Theta\left(\frac{y + \hat{A}}{\sqrt{4\hat{A}}}\right) \log \Theta\left(\frac{y + \hat{A}}{\sqrt{4\hat{A}}}\right) \right] \right\}$$
(3.1.15)

Thus the equations for  $\varphi_K$ , in the high-dimensional expansion, are

$$\hat{\varphi} = \frac{\log \frac{d}{\hat{A}} - 1 + \frac{2}{d} \left[ 1 - \log(\sqrt{\pi d^3} \hat{\varphi}) \right]}{1 + \int_{-\infty}^{\infty} dy e^y \Theta\left(\frac{y + \hat{A}}{\sqrt{4\hat{A}}}\right) \log \Theta\left(\frac{y + \hat{A}}{\sqrt{4\hat{A}}}\right)} \quad \text{and} \quad 1 = \hat{\varphi} F_1(\hat{A}) = \hat{\varphi} \sqrt{\frac{\hat{A}}{\pi}} \int_{-\infty}^{\infty} dt t e^{-t^2} \log \Theta\left(t + \sqrt{\hat{A}}\right)$$
(3.1.16)

At the first order in  $\hat{A}$ , the second equation behaves as  $\hat{\varphi} \sim \hat{A}^{-1/2}$ . So, with the first equation, we get at the first order in the dimension  $\hat{\varphi}_K \sim \log d$  and thus,  $\hat{A}_K \sim (\log d)^{-2}$ , which is consistent with the first order expansion in  $\hat{A}$ .

Using the expression of  $q_A$  and  $S_{liq}$ , we can derive also the expression of  $\Sigma_j$  from (2.5.8),

$$\Sigma_{j}(\alpha,\varphi) = S_{liq}(\varphi) - \frac{d}{2}[\log(2\pi\alpha) + 1] + 2^{d-1}d\varphi g_{liq}(1,\varphi) \int_{0}^{1} dr r^{d-1} e^{-\frac{(r-1)^{2}}{4\alpha}}$$

$$= 1 - \log(\sqrt{\pi d^{3}}\hat{\varphi}) + \frac{d}{2} \left\{ \log\frac{d}{\hat{\alpha}} - \hat{\varphi} \left[ 1 - \int_{0}^{\infty} dy e^{-y - \frac{y^{2}}{4\hat{\alpha}}} \right] \right\}$$

$$= 1 - \log(\sqrt{\pi d^{3}}\hat{\varphi}) + \frac{d}{2} \left\{ \log\frac{d}{\hat{\alpha}} - \hat{\varphi} \left[ 1 - \sqrt{4\pi\hat{\alpha}}e^{\hat{\alpha}}\Theta(-\sqrt{\hat{\alpha}}) \right] \right\}$$
(3.1.17)

Thus the equations for  $\varphi_{GCP}$ , in the high-dimensional expansion, are

$$\hat{\varphi} = \frac{\log \frac{d}{\hat{\alpha}} + \frac{d}{2} \left[ 1 - \log(\sqrt{\pi d^3} \hat{\varphi}) \right]}{1 - \sqrt{4\pi \hat{\alpha}} e^{\hat{\alpha}} \Theta(-\sqrt{\hat{\alpha}})} \quad \text{and} \quad 1 = \hat{\varphi} F_0(\hat{\alpha}) = -\hat{\alpha} + (1 + 2\hat{\alpha}) \sqrt{\pi \hat{\alpha}} e^{\hat{\alpha}} \Theta\left(-\sqrt{\hat{\alpha}}\right)$$
(3.1.18)

At the first order in  $\hat{\alpha}$ , the second equation behaves as  $\hat{\varphi} = \frac{2}{\sqrt{\pi \hat{\alpha}}} \sim \hat{\alpha}^{-1/2}$ . So, with the first equation, we get at the first order in the dimension  $\hat{\varphi}_{GCP} = \log d$  and thus,  $\hat{\alpha} = \frac{4}{\pi (\log d)^2}$ , which is consistent with the first order expansion in  $\hat{\alpha}$ .

# 3.2 Small cage expansion

As seen in the previous section, the cage A decreases with the dimension, so in this section, we will derive the complexities  $\Sigma_{eq}$  and  $\Sigma_j$  at the first order in  $\sqrt{A}$  to obtain the equation of  $\varphi_K$  and  $\varphi_{GCP}$  respectively.

#### **3.2.1** Derivation of $\Sigma_{eq}$ and $\varphi_K$

Before computing the expansion of  $\Sigma_{eq}$ , we need to compute the expansion at the first order in  $\sqrt{A}$  of  $q_A(r,\varphi)$  and  $\frac{\partial q_A}{\partial A}(r,\varphi)$ . First, the expansion of Bessel functions is

$$e^{-x}\sqrt{2\pi x}I_n(x) = 1 + \frac{1-n^2}{2x} + \frac{(n+1)^2}{8x^2}(2n^2 + 2n + 3) + \mathcal{O}(x^3) \Rightarrow e^{-\frac{ru}{2A}}\sqrt{\pi \frac{ru}{A}}I_n\left(\frac{ru}{2A}\right) = 1 + \frac{1-n^2}{ru}A + \mathcal{O}(A^2)$$
(3.2.1)

When  $r > 1 + \mathcal{O}(\sqrt{A})$ , we can take the behaviour of the Gaussian as a  $\delta$  function (because  $g_{liq}$  is derivable) and thus, we get at the first order in A,

$$q_{A}(r,\varphi) = g_{liq}(r,\varphi) + \mathcal{O}(A)$$

$$\widetilde{q_{A}}(r,\varphi) = -g_{liq}(r,\varphi)\log g_{liq}(r,\varphi) + \mathcal{O}(A)$$

$$\frac{\partial q_{A}}{\partial A}(r,\varphi) = g_{liq}(r,\varphi)\frac{1}{2A^{2}}\left[\left(r^{2} - dA\right) \cdot \left(1 + \frac{1 - (d/2 - 1)^{2}}{r^{2}}A\right) - r^{2} \cdot \left(1 + \frac{1 - (d/2)^{2}}{r^{2}}A\right) + \mathcal{O}(A^{2})\right]$$

$$= -\frac{1}{2A}g_{liq}(r,\varphi) + \mathcal{O}(1)$$
(3.2.2)

and when  $r < 1 - \mathcal{O}(\sqrt{A})$ , with the same argument and from  $g_{liq}(r,\varphi) = 0$ ,  $q_A(r,\varphi) = 0$ ,  $\widetilde{q_A}(r,\varphi) = 0$  and  $\frac{\partial q_A}{\partial A}(r,\varphi) = 0$ . For  $|r-1| < \mathcal{O}(\sqrt{A})$ , we can take the usual changes of variables  $t = \frac{r-1}{\sqrt{4A}}$  and  $s = \frac{u-1}{\sqrt{4A}}$ , at the first order in A, we get

$$q_{A}(t,\varphi) = \sqrt{4A} \int_{0}^{\infty} ds g_{liq} (1 + s\sqrt{A}, \varphi) \left(\frac{1 + s\sqrt{A}}{1 + t\sqrt{A}}\right)^{\frac{d-1}{2}} \frac{e^{-(s-t)^{2}}}{\sqrt{4\pi A}} [1 + \mathcal{O}(A)]$$

$$= g_{liq}(1,\varphi) \int_{-\infty}^{t} \frac{ds}{\sqrt{\pi}} e^{-s^{2}} + \mathcal{O}(\sqrt{A}) = g_{liq}(1,\varphi)\Theta(t) + \mathcal{O}(\sqrt{A})$$

$$\widetilde{q}_{A}(t,\varphi) = -g_{liq}(1,\varphi) \log g_{liq}(1,\varphi)\Theta(t) + \mathcal{O}(\sqrt{A})$$

$$\frac{\partial q_{A}}{\partial A}(t,\varphi) = \frac{g_{liq}(1,\varphi)}{A} \int_{-\infty}^{t} \frac{ds}{\sqrt{\pi}} (s^{2} - \frac{1}{2}) e^{-s^{2}} + \mathcal{O}(\frac{1}{\sqrt{A}}) = -\frac{g_{liq}(1,\varphi)}{2\sqrt{\pi}A} t e^{-t^{2}} + \mathcal{O}(\frac{1}{\sqrt{A}})$$

$$(3.2.3)$$

with the same kind of calculation for the three computations, but taking the first order of Bessel function into account for the  $\frac{\partial q_A}{\partial A}$  one.

From the equation over A in (2.4.2), we get at the first order in  $\sqrt{A}$ , with  $\hat{\varphi} = \frac{2^d \varphi}{d}$ ,

$$1 = -\hat{\varphi}dA \int_{1-\mathcal{O}(\sqrt{A})}^{1+\mathcal{O}(\sqrt{A})} dr r^{d-1} \frac{\partial q_A}{\partial A}(r,\varphi) \log q_A(r,\varphi) = \hat{\varphi}d\sqrt{4A} \int_{-\infty}^{+\infty} dt \frac{g_{liq}(1,\varphi)}{2\sqrt{\pi}} t e^{-t^2} \log(g_{liq}(1,\varphi)\Theta(t))$$

$$= \hat{\varphi}d\sqrt{A}g_{liq}(1,\varphi) \int_{-\infty}^{+\infty} dt t \frac{d\Theta}{dt}(t) \log \Theta(t) = -\hat{\varphi}d\sqrt{A}g_{liq}(1,\varphi) \int_{-\infty}^{+\infty} dt \Theta(t) \log \Theta(t) = \hat{\varphi}d\sqrt{A}g_{liq}(1,\varphi)Q_0 \qquad (3.2.4)$$

$$\Rightarrow \sqrt{A} = \frac{1}{\hat{\varphi}dg_{liq}(1,\varphi)Q_0} \text{ with } Q_0 = -\int_{-\infty}^{+\infty} dt \Theta(t) \log \Theta(t) = 0.63865692$$

From this value of A and the equation of  $\Sigma_{eq}$  in (2.4.2), we get its expression at the first order in  $\sqrt{A}$ ,

$$\Sigma_{eq}(A,\varphi) = S_{liq}(\varphi) - \frac{d}{2}\log(2\pi A) - d - \frac{1}{2}\hat{\varphi}d^2 \int_{1-\mathcal{O}(\sqrt{A})}^{1+\mathcal{O}(\sqrt{A})} dr r^{d-1}[q_A(r,\varphi)\log q_A(r,\varphi) + \widetilde{q_A}(r,\varphi)]$$

$$= S_{liq}(\varphi) - d\log(\sqrt{2\pi A}) - d - \hat{\varphi}d^2\sqrt{A}\int_{-\infty}^{+\infty} dt g_{liq}(1,\varphi)\Theta(t)[\log(g_{liq}(1,\varphi)\Theta(t)) - \log g_{liq}(1,\varphi)]$$

$$= S_{liq}(\varphi) - d\log(\sqrt{2\pi A}) - d + \hat{\varphi}d^2\sqrt{A}g_{liq}(1,\varphi)Q_0$$
(3.2.5)

$$\Sigma_{eq}(\varphi) = S_{liq}(\varphi) - d\log\left(\frac{\sqrt{2\pi}}{\hat{\varphi}dg_{liq}(1,\varphi)Q_0}\right)$$
(3.2.6)

The value of  $\varphi_K$  in this expansion is obtained by solving  $\Sigma_{eq}(\varphi) = 0$  with the equation (3.2.6) implicit in  $\varphi$  but with no dependance in A. This result is the same than the one computed in [PZ10].

### **3.2.2** Derivation of $\Sigma_i$ and $\varphi_{GCP}$

From the equation over  $\alpha$  in (2.5.8), we get at the first order in  $\sqrt{\alpha}$ ,

$$1 = \hat{\varphi} dg_{liq}(1, \varphi) \int_{0}^{1} dr r^{d-1} \frac{(r-1)^{2}}{4\alpha} e^{-\frac{(r-1)^{2}}{4\alpha}} = \hat{\varphi} dg_{liq}(1, \varphi) \sqrt{4\alpha} \int_{0}^{\infty} dt t^{2} e^{-t^{2}} \Rightarrow \sqrt{\pi \alpha} = \frac{2}{dg_{liq}(1, \varphi)\hat{\varphi}}$$
(3.2.7)

with the usual change of variables  $t = \frac{r-1}{\sqrt{4\alpha}}$  and  $\hat{\varphi} = \frac{2^d \varphi}{d}$ .

From this value of  $\alpha$  and the equation of  $\Sigma_j$  in (2.5.8), we get its expression at the first order in  $\sqrt{\alpha}$ ,

$$\Sigma_{j}(\alpha,\varphi) = S_{liq}(\varphi) - \frac{d}{2}[\log(2\pi\alpha) + 1] + \frac{1}{2}\hat{\varphi}d^{2}g_{liq}(1,\varphi) \int_{0}^{1} dr r^{d-1} e^{-\frac{(r-1)^{2}}{4\alpha}}$$

$$= S_{liq}(\varphi) - d\log(\sqrt{2\pi\alpha}) - \frac{d}{2} + \hat{\varphi}d^{2}g_{liq}(1,\varphi)\sqrt{\alpha} \int_{0}^{\infty} dt e^{-t^{2}}$$
(3.2.8)

$$\Sigma_{j}(\varphi) = S_{liq}(\varphi) - d\log\left(\frac{2\sqrt{2}}{dg_{liq}(1,\varphi)\hat{\varphi}}\right) + \frac{d}{2}$$
(3.2.9)

The value of  $\varphi_{GCP}$  in this expansion is obtained by solving  $\Sigma_j(\varphi) = 0$  with the equation (3.2.9) implicit in  $\varphi$  but with no dependance in  $\alpha$ . This result is the same than the one computed in [PZ10].

#### 3.3 Computation for finite dimension

The numerical resolution of equations of  $\varphi_d$ ,  $\varphi_K$ ,  $\varphi_{th}$  and  $\varphi_{GCP}$  needs the computation of the pair correlation  $g_{liq}(r,\varphi)$  by an iterative algorithm and needs also some other basic algorithm. After having given this algorithm, I will show the results for the different densities.

### **3.3.1** Algorithm for $g_{liq}(r,\varphi)$

The equation to get  $g_{liq}(r,\varphi)$ , derived in the section 1.1, can be reexpressed for the hard-sphere potential. We define as straightforward function  $\gamma(r) = h(r) - c(r)$ . The Hyper Netted Chain equation (1.1.23) becomes

$$c(r) = e^{-\beta v(r)} e^{h(r) - c(r)} - 1 - [h(r) - c(r)] = e^{\gamma(r) - \beta v(r)} - 1 - \gamma(r) = \begin{cases} -1 - \gamma(r) & r < 1 \\ e^{\gamma(r)} - 1 - \gamma(r) & r > 1 \end{cases}$$
(3.3.1)

the Percus-Yevick equation (1.1.26) becomes

$$c(r) = e^{-\beta v(r)} [1 + h(r) - c(r)] - 1 - [h(r) - c(r)] = e^{-\beta v(r)} [1 + \gamma(r)] - 1 - \gamma(r) = \begin{cases} -1 - \gamma(r) & r < 1 \\ 0 & r > 1 \end{cases}$$
(3.3.2)

and the Ornstein-Zernike equation (1.1.21) becomes

$$\hat{\gamma}(k) = \hat{h}(k) - \hat{c}(k) = \frac{\hat{c}(k)}{1 - \rho \hat{c}(k)} - \hat{c}(k) = \frac{\rho \hat{c}(k)^2}{1 - \rho \hat{c}(k)}$$
(3.3.3)

#### Discrete Fourier transformation

To solve these equation iteratively, we need to perform a discrete Fourier transformation in d dimension. The function c and  $\gamma$  are radial thus, in this case, we need to perform a Hankel transformation such that (for any radial function f which can represent c or  $\gamma$ ),

$$\hat{f}(k) = \frac{(2\pi)^{\frac{d}{2}}}{k^{\frac{d}{2}-1}} \int_0^\infty dr r^{\frac{d}{2}} J_{\frac{d}{2}-1}(kr) f(r), \quad f(r) = \frac{(2\pi)^{-\frac{d}{2}}}{r^{\frac{d}{2}-1}} \int_0^\infty dk k^{\frac{d}{2}} J_{\frac{d}{2}-1}(kr) \hat{f}(k)$$
(3.3.4)

To simplify these equations, we can define new functions  $F(r) = r^{\frac{d}{2}-1}f(r)$  and  $\hat{F}(k) = k^{\frac{d}{2}-1}\hat{f}(k)$ , we get thus

$$\hat{F}(k) = (2\pi)^{\frac{d}{2}} \int_0^\infty dr r J_{\frac{d}{2}-1}(kr) F(r), \quad F(r) = (2\pi)^{-\frac{d}{2}} \int_0^\infty dk k J_{\frac{d}{2}-1}(kr) \hat{F}(k)$$
(3.3.5)

The orthogonality of Hankel transformations

$$\int_{0}^{\infty} dr r J_{\frac{d}{2}-1}(kr) J_{\frac{d}{2}-1}(k'r) = \frac{\delta(k-k')}{k}$$
(3.3.6)

permits to assure the consistency of previous equations. We need now to discretize these equations on a grid of N elements with r in an interval  $[0, R_{max}]$  and k in an interval  $[0, K_{max}]$  to solve the problem numerically. But, we need to preserve this orthogonality! A good way to do this is to cut the intervals in the zeros of the  $(\frac{d}{2}-1)^{th}$  order Bessel function. We call  $\lambda_i$  the  $i^{th}$  zero of  $J_{\frac{d}{2}-1}$ , such that  $\lambda_i \neq 0$ . We take thus  $r_i = \frac{\lambda_i}{K_{max}}$  and  $k_i = \frac{\lambda_i}{R_{max}}$ .  $R_{max}$  and  $K_{max}$ are thus related as  $R_{max} \cdot K_{max} = \lambda_N^2$ . The equations (3.3.5) transform as

$$\hat{F}(k_i) = \sum_{j=1}^{N} (RK)_{ij} F(r_j), \quad (RK)_{ij} = \frac{2(2\pi)^{\frac{d}{2}}}{K_{max}^2} \frac{J_{\frac{d}{2}-1}(k_i r_j)}{J_{\frac{d}{2}}(K_{max} r_j)^2}$$

$$F(r_i) = \sum_{j=1}^{N} (KR)_{ij} \hat{F}(r_j), \quad (KR)_{ij} = \frac{2(2\pi)^{-\frac{d}{2}}}{R_{max}^2} \frac{J_{\frac{d}{2}-1}(k_j r_i)}{J_{\frac{d}{2}}(R_{max} k_j)^2}$$
(3.3.7)

When N is large, the continuous and the discrete version are equivalent, using the asymptotic expression

$$J_{\frac{d}{2}}(x) = \sqrt{\frac{2}{\pi x}}\cos(x - (d - 1)\frac{\pi}{4}) \text{ and } \lambda_i = (i + \frac{d - 3}{4})\pi \Rightarrow J_{\frac{d}{2}}(K_{max}r_j)^2 \sim \frac{2}{\pi K_{max}r_i} \text{ and } J_{\frac{d}{2}}(R_{max}k_j)^2 \sim \frac{2}{\pi R_{max}k_j}$$
(3.3.8)

From this, we get the equivalence of formulas

$$\hat{F}(k_i) \sim \frac{\pi (2\pi)^{\frac{d}{2}}}{K_{max}} \sum_{j=1}^{N} r_j F(r_j) J_{\frac{d}{2}-1}(k_i r_j) \sim (2\pi)^{\frac{d}{2}} \int_0^{R_{max}} dr r J_{\frac{d}{2}-1}(k_j r) F(r)$$

$$F(r_i) \sim \frac{\pi (2\pi)^{-\frac{d}{2}}}{R_{max}} \sum_{j=1}^{N} k_j \hat{F}(k_j) J_{\frac{d}{2}-1}(k_j r_i) \sim (2\pi)^{-\frac{d}{2}} \int_0^{K_{max}} dk k J_{\frac{d}{2}-1}(k r_i) \hat{F}(k)$$
(3.3.9)

and the consistency property, using  $x_i = \lambda_i/\lambda_N$ 

$$F(r_{i}) \sim \frac{\pi^{2}}{\lambda_{N}} \sum_{j,l} r_{l} k_{j} F(r_{l}) J_{\frac{d}{2}-1}(k_{l} r_{j}) J_{\frac{d}{2}-1}(k_{j} r_{i}) = \pi^{2} \sum_{j,l} \lambda_{l} x_{j} F(r_{l}) J_{\frac{d}{2}-1}(\lambda_{l} x_{j}) J_{\frac{d}{2}-1}(\lambda_{i} x_{j})$$

$$\sim \sum_{l} F(r_{l}) \lambda_{l} \int_{0}^{1} dx x J_{\frac{d}{2}-1}(\lambda_{l} x) J_{\frac{d}{2}-1}(\lambda_{i} x) = \sum_{l} F(r_{l}) \delta_{il}$$
(3.3.10)

#### Algorithm for $g_{liq}$

For the Hyper Netted Chain and the Percus-Yevick approximation, the next iterative algorithm is applied to get  $g_{liq}(r)$ 

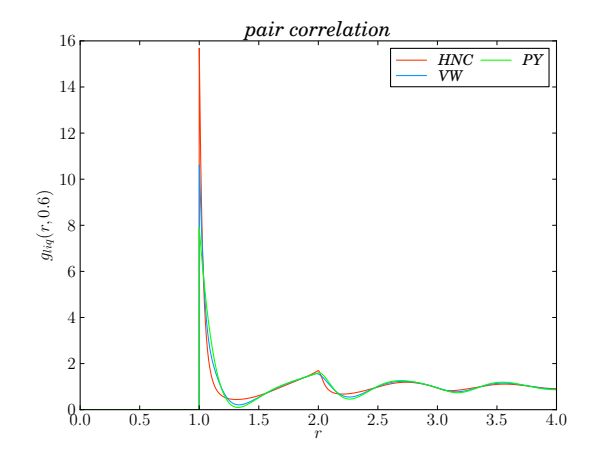
- 1. Give some arguments : d, N,  $R_{max}$  and  $\rho$ .
- 2. Evaluate  $\{\lambda_i\}$ ,  $K_{max}$ ,  $\{r_i\}$ ,  $\{k_i\}$ ,  $\{RK\}$  and  $\{KR\}$  and keep them in memory (dependence on d, N,  $R_{max}$  only).
- 3. Take an initial form of  $\gamma$ : here we use  $\gamma(r) = 0$ .
- 4. Do a recursive sequence to evaluate  $\gamma$  and c:
  - (a) Evaluate c from HNC or PY equation.
  - (b) Evaluate  $C(r_i) = r_i^{\frac{d}{2}-1}c(r_i)$ ,  $\hat{C}(k_i)$  with (RK) from (3.3.7) and  $\hat{c}(k_i) = k_i^{1-\frac{d}{2}}\hat{C}(k_i)$ .
  - (c) Evaluate  $\hat{\gamma}$  with OZ equation.
  - (d) Evaluate  $\hat{\Gamma}(k_i) = k_i^{\frac{d}{2}-1} \hat{\gamma}(k_i)$ ,  $\Gamma(r_i)$  with (KR) from (3.3.7) and  $\gamma(r_i) = r_i^{1-\frac{d}{2}} \Gamma(r_i)$ .
  - (e) Guess a new value of  $\gamma$  from  $\gamma(r) = (1 \alpha)\gamma_{old}(r) + \alpha\gamma_{new}(r)$ , for  $\alpha$  small to have a convergence of the algorithm. A faster method consists to use the DIIS algorithm which takes the value of  $\gamma$  in last n steps.
  - (f) The iteration stops when  $|\gamma_{old} \gamma_{new}| < 10^{-10}$ .
- 5. Return  $g(r) = \gamma(r) + c(r) + 1$  as a linear interpolation of its discretized values, with a precaution at the discontinuity in r = 1: g(r < 0) = 0 and  $g(1^+)$  is evaluated with the next linear interpolation.

For the Verlet-Weis approximation, the algorithm is applied to find  $q_{PY}$  at  $\varphi^*$  and the pair correlation function is obtained with the equation (1.1.31).

For a computer of 3.5 GHz CPU, the initialization step 2, costs about 30 seconds and the converging sequence needs 10 seconds for N = 3000, and for a C++ code using the GSL library to compute Bessel functions.

#### Results in dimension 3

In dimension 3, as in all dimensions, the pair correlation decreases through  $\theta(r-1)$  for a small density. In the special case of the third dimension, the value in 1 is bigger for the HNC approximation and smaller for the PY approximation than for the VW one.



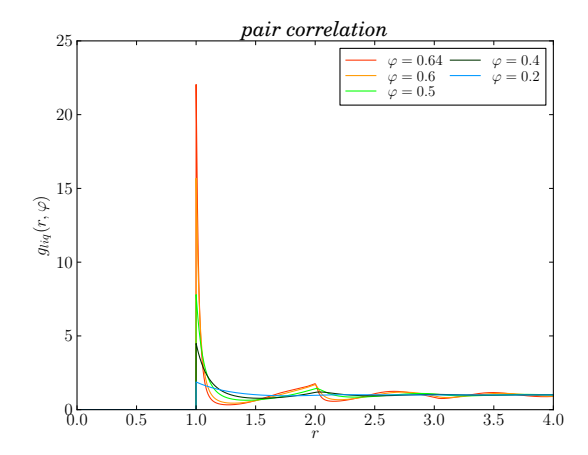


Figure 6 – Pair correlation for different approximation at d=3 for  $\varphi=0.6$ 

Figure 7 – Pair correlation in HNC approximation for d=3

#### 3.3.2 Algorithm to compute the densities

To compute the different densities, we need three particular algorithms to integrate, to inverse a function and to compute the maximum of a function with an efficiently way due to the difficulty to evaluate the function.

#### Integration algorithm

After taking the change of variable of (t,s), we need just to integrate a Gaussian function centered in zero multiplied by a constant sign function which evolves slowly. We can thus integrate, starting from the center of the integral until that the value of the function becomes negligeable (less than  $10^{-10}$  of the value of the integral). The integral of a function f between a and b is calculated by discretizing the interval into N subinterval of constant size  $dx = \frac{b-a}{N}$ . The trapeze method gives

$$\int_{a}^{b} dx f(x) = \frac{f(a)}{2} + \sum_{i=1}^{N-1} f(a+i \cdot dx) + \frac{f(b)}{2} + \mathcal{O}(dx^{2})$$
(3.3.11)

The Simpson method, more precise, gives for an even N

$$\int_{a}^{b} dx f(x) = \frac{f(a)}{3} + \frac{2}{3} \sum_{i=0}^{N/2-1} f(a + (2i+1) \cdot dx) + \frac{4}{3} \sum_{i=1}^{N/2-1} f(a+2i \cdot dx) + \frac{f(b)}{3} + \mathcal{O}(dx^{3})$$
(3.3.12)

# Inversion algorithm

To calculate the inverse of a function f at  $\alpha$ , i.e. find x such that  $f(x) = \alpha$ , we compute the bissection algorithm in  $g(x) = f(x) - \alpha = 0$ . For n evaluation of f, the gain of precision  $\epsilon$  of the solution is  $2^{1-n}$  starting from an interval [a,b]. We have thus  $n = 1 - \log_2 \epsilon$ . The bissection agorithm is given by:

- 1. Evaluate and keep in memory g(a) and g(b).
- 2. If  $g(a)\cdot g(b)<0$  and while  $\frac{2(b-a)}{a+b}<\epsilon$  do
  - (a) Evaluate and keep in memory  $g(c = \frac{a+b}{2})$ .
  - (b) If  $g(a) \cdot g(c) < 0$  then  $\{b := c \text{ and } g(b) := g(c)\}$  else  $\{a := c \text{ and } g(a) := g(c)\}$ .
- 3. Return  $\frac{a+b}{2}$ .

#### Maximum algorithm

To calculate the unique maximum of a function f between a and b, the most efficient algorithm gives a precision  $\epsilon \sim 3^{2-n} \iff n=2+\log_3 \epsilon$  with n the number of evalutation of f. The algorithm used is

1. Evaluate and keep in memory f(a) and f(b).

- 2. Evaluate and keep in memory  $f(c = \frac{2a+b}{3})$  and  $f(d = \frac{a+2b}{3})$ .
- 3. While  $\frac{2(b-a)}{a+b} < \epsilon$  do
  - (a) If f(c) > f(d) then  $\{b := d, f(b) := f(d), m := c \text{ and } f(m) := f(c)\}$  else  $\{a := c, f(a) := f(c), m := d \text{ and } f(m) := f(d)\}.$
  - (b) Take the biggest interval between [a, m] and [m, b] and cut this one in the middle in the new point n.
  - (c) Evaluate and keep in memory f(n).
  - (d) Change by pair the name of m and n and the function values into c and d such that c < d.
- 4. Return  $\frac{f(a)+f(b)}{2}$ .

#### 3.3.3 Numerical results for densities

Our approach permits us to get  $\varphi_d$ ,  $\varphi_K$ ,  $\varphi_{th}$  and  $\varphi_{GCP}$  at all dimension. We recover the asymptotic limit at  $d \to \infty$  where the theory is exact. The comparisons with the experimental results and simulations, which can be found in [CIPZ11], are correct. Here, we will find these results for Hyper Netted Chain (HNC), Percus-Yevick (PY) and Verlet-Weis (VW) approximations of the liquid pair correlation and entropy. We will present also the results in a modified Verlet-Weis approximation (VWfit), where we use the fitted  $\mathcal{A}_d$  coefficients from [CIPZ11] for the hard sphere phase diagram until dimension 12.

#### Results for the equilibrium line

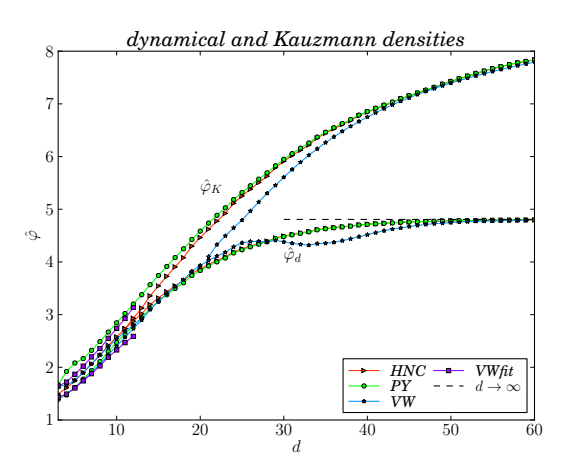


FIGURE 8 – Dimensional behaviour of dynamical  $(\varphi_d)$  and Kauzmann  $(\varphi_k)$  densities for different approximations. In dashed line, the high dimension result.

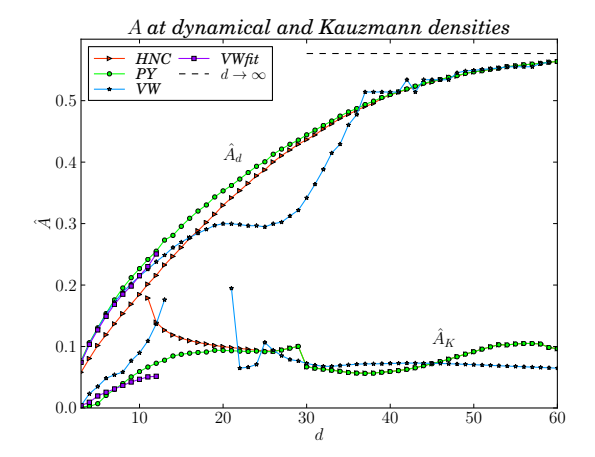


FIGURE 9 – Dimensional behaviour of  $\hat{A}$  at the dynamical  $(\varphi_d)$  and Kauzmann  $(\varphi_k)$  densities for different approximations. In dashed line, the high dimension result.

For all approximations, the scaled dynamical packing fraction  $\hat{\varphi}_d$  converges through the high dimensional value 4.8067787 (Fig. 8), as the scaled dynamical cage  $\hat{A}_d$  which converges through 0.5766799 (Fig. 9).

For the HNC approximation, the Kauzmann packing fraction  $\varphi_K$  does not exists at dimension lower than 12. This comes from the fact that the complexity at the dynamical packing fraction is already negative. The same effect occurs for the VW approximation for a dimension between 14 and 20 included (Fig. 10). In these cases, we can consider that  $\varphi_d = \varphi_K$ . Despite this effect, the value of the scaled Kauzmann packing fraction  $\hat{\varphi}_K$  converges to the same value for all approximations which seems to continue to increase, the behaviour that the high-dimensional behaviour suggests (Fig. 8). The same kind of convergence is also seen for the Kauzmann scaled cage  $\hat{A}_k$  (Fig. 9).

The problem of continuity of the complexity at some dimension in the figure 10 comes from the evaluation of Bessel functions for a large arguments, i.e. in our case for  $A < 10^{-4} - 10^{-5}$ . This problem only occurs in the  $\varphi_K$  derivation and should be solved to get better values. This also brings the jumps in the figure 9.

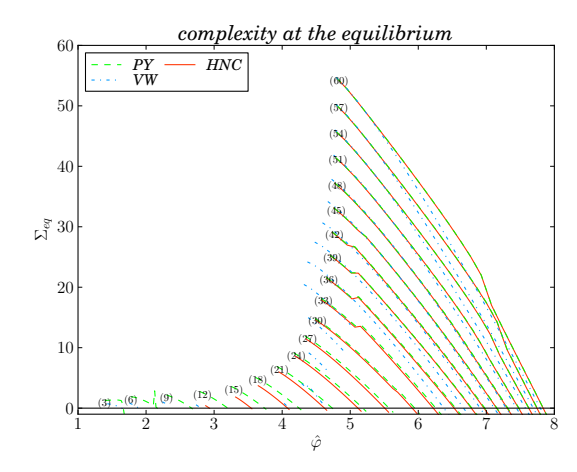
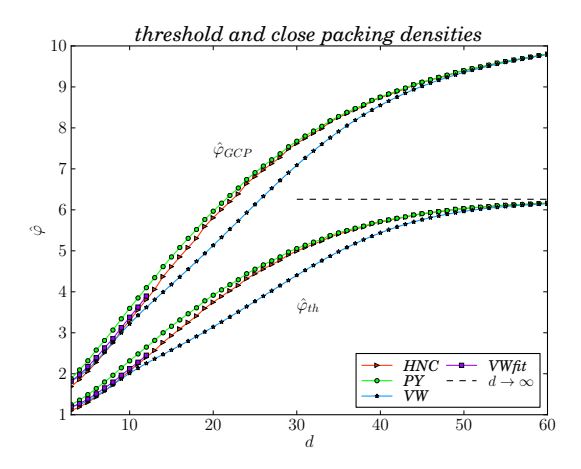


FIGURE 10 – The complexity at the equilibrium versus the scaled packing fraction for different dimensions.

#### Results for the jamming line



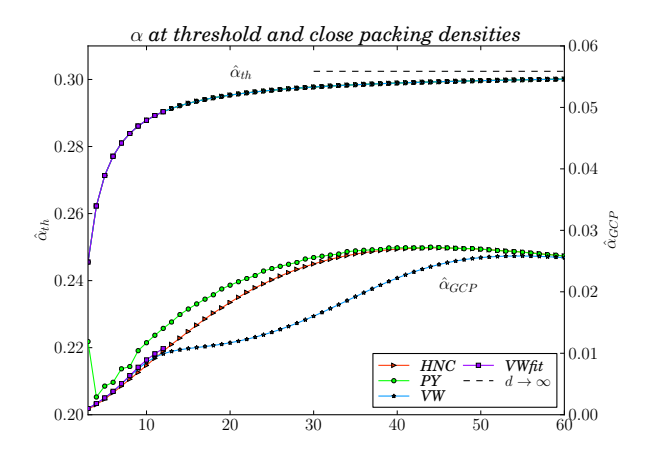


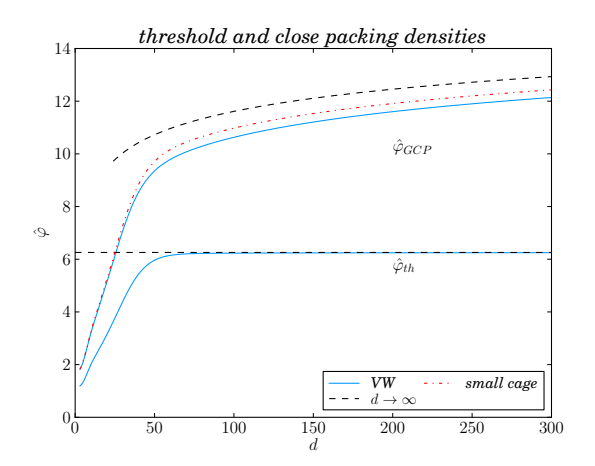
FIGURE 11 – Dimensional behaviour of threshold  $(\varphi_{th})$  and close packing  $(\varphi_{GCP})$  densities for different approximations. In dashed line, the high dimension result.

FIGURE 12 – Dimensional behaviour of  $\hat{\alpha}$  at the threshold  $(\varphi_{th})$  and close packing  $(\varphi_{GCP})$  densities for different approximations. In dashed line, the high dimension result.

For all approximations, the scaled threshold packing fraction  $\hat{\varphi}_{th}$  converges through the high dimensional value 6.2581221 (Fig. 11), as the scaled threshold cage  $\hat{\alpha}_{th}$  which converges through 0.3024338 (Fig. 12).

At the contrary of equilibrium line, the complexity at the jamming is always positive at the threshold value for all approximations (Fig. 14). Thus the scaled close packing fraction  $\hat{\varphi}_{GCP}$  always exists. For all approximation, the values converges to a same one. The increasing behaviour follows the high dimensional result as well as for  $\hat{\varphi}_{GCP}$  (Fig. 11) than for  $\hat{\alpha}_{GCP}$  (Fig. 12).

The VW results, the small cage behaviour and the asymptotic behaviour are shown for bigger dimension in the figure 13.



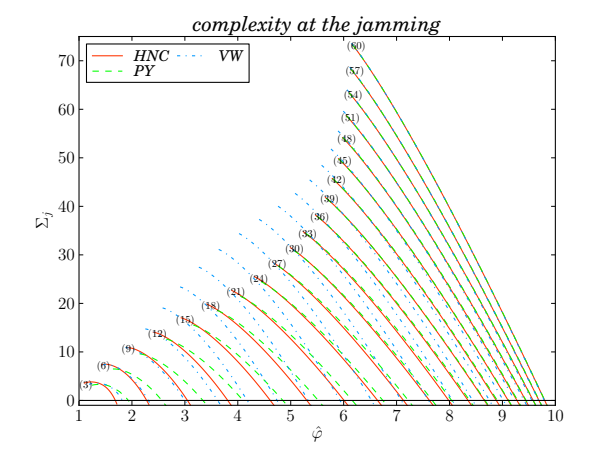


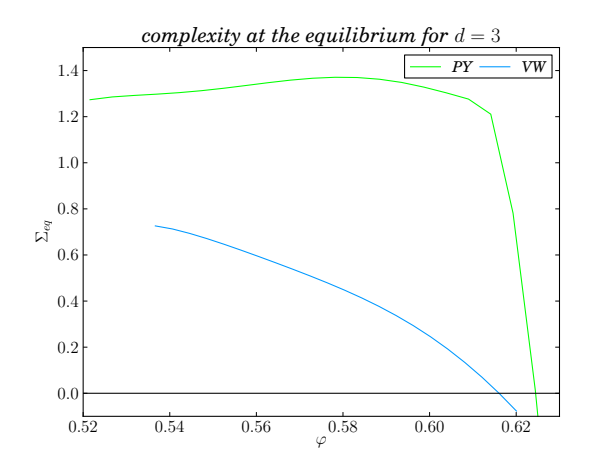
FIGURE 13 – Threshold  $(\varphi_{th})$  and close packing  $(\varphi_{GCP})$  densities for many approximations until d = 300.

FIGURE 14 – The complexity at the jamming versus the scaled packing fraction for different dimensions.

#### Summary of results for d = 3

In this section, I will summarize the most important result of our approch: we can get a good result for the phase transition points in dimension 3. In the next table, we can found the results for all approximations, the small cage expansion, already done in [PZ10] and the results of simulation done in [CIPZ11]. Let me remind that the Kauzmann packing fraction does not exist for the HNC approximation, because the complexity at the dynamical packing fraction is negative... The behaviour of the complexity is given in the figure 15 for the equilibrium and in the figure 16 for the jamming.

Approximations/densities	$\varphi_d$	$\varphi_K$	$\varphi_{th}$	$\varphi_{GCP}$
HNC	0.559609	-	0.412506	0.632244
PY	0.521587	0.624414	0.467388	0.705571
VW=VWfit	0.536662	0.616089	0.446276	0.682338
Small Cage (CS)	-	0.617616	-	0.683657
[CIPZ11]	0.571	-	0.651	-



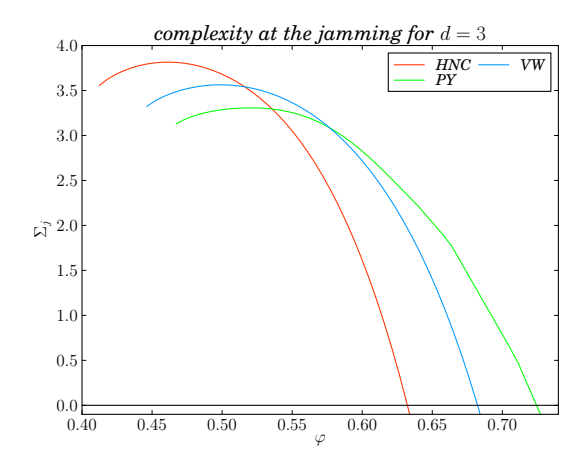


FIGURE 15 – The complexity at the equilibrium versus the packing fraction at dimension 3.

FIGURE 16 – The complexity at the jamming versus the packing fraction at dimension 3.

# 4 The non-ergodicity factor

We define the non-ergodicity factor, as for the liquids,

$$f(k) = \lim_{t \to \infty} \frac{S(k,t)}{S(k)} \tag{4.0.13}$$

where  $S(q) = \langle \frac{1}{N} \rho(q) \rho(-q) \rangle$  the static structure factor and  $S(q,t) = \langle \frac{1}{N} \rho(q,t) \rho(-q,0) \rangle$  the dynamic structure factor. From this definition and the replica method, we get

$$\lim_{t \to \infty} S(q,t) = \frac{1}{N} \overline{\rho_a(q)\rho_a(-q)} = \rho \tilde{h}(q) = \int dr e^{-iqr} \rho_{ab}(r)$$

$$\rho_{ab}(x,y) = \frac{1}{N} \langle \delta(x-x_a)\delta(y-y_a) \rangle = \frac{1}{N} \overline{\rho_a(x)\rho_b(y)}$$
(4.0.14)

From the Gaussian form of density function (2.1.2) and the form of the correlation (2.1.3), rewritten as

$$\rho_{ab}(\bar{x}, \bar{y}) = \rho(\bar{x})\rho(\bar{y}) \prod_{a=1}^{m} g_{liq}(|x_a - y_a|)^{\frac{1}{m}}$$
(4.0.15)

we can derive the expression of  $\rho_{12}(x-y)$  which decomposes into two parts : 1 and 2 belong to the same replica (interaction) or they belong to different replicas (interreplica interaction). So, we get

$$\rho_{12}(x-y) = \frac{1}{N} \int dx_3 ... dx_m d\bar{y} \rho^{(1)}(x, y, x_3, ..., x_m) \rho^{(1)}(\bar{y}) + \int dx_2 ... dx_m dy_1 dy_3 ... dy_m \rho^{(2)}(x, x_2, ..., x_m; y_1, y, y_3, ..., y_m) 
= \rho \int x_3 ... dx_m \int dX \prod_{a=1}^m \gamma_A(x_a - X) + \rho^2 \int dx_2 ... dx_m dy_1 dy_3 ... dy_m \int dX dY \prod_{a=1}^m [\gamma_A(x_a - X)\gamma_A(y_a - Y)g_{liq}(x_a - y_a)^{\frac{1}{m}}] 
= \rho \int dX \gamma_A(x - X)\gamma_A(y - X) + \rho^2 \int dX dY dx_2 dy_1 \gamma_A(x - X)\gamma_A(y_1 - Y)g_{liq}(x - y_1)^{\frac{1}{m}} 
\gamma_A(x_2 - X)\gamma_A(y - Y)g_{liq}(x_2 - y)^{\frac{1}{m}} q_A(X - Y)^{m-2}$$
(4.0.16)

We can write this equation, for m=1, in a diagrammatic expression as

$$\rho_{12}(x-y) = \rho \gamma_{2A}(x-y) + \rho^2 \begin{cases} x & \gamma_A & X & \gamma_A & x_2 \\ y & 1/q_A & g \\ y_1 & \gamma_A & V & \gamma_A & y \end{cases}$$

$$(4.0.17)$$

From the Feynman rules, we get in the momentum space

$$\hat{\rho}_{12}(q) = \rho e^{-Aq^2} + \rho^2 \int \frac{dk_1}{(2\pi)^d} \frac{dk_2}{(2\pi)^d} \hat{\gamma}_A(k_1) \hat{\gamma}_A(q - k_1) \hat{\gamma}_A(q - k_2) \hat{g}_{liq}(k_1) \hat{g}_{liq}(k_2) \hat{q}_A^{-1}(q - k_1 - k_2)$$
(4.0.18)

where  $\hat{\gamma}_A(k) = e^{-Ak^2/2}$ ,  $\hat{q}_A^{-1}$  the Fourier transform of  $1/q_A$  and  $\hat{g}_{liq}(k) = \hat{h}_{liq}(k) + (2\pi)^d \delta(k)$ .

From this we get the expression for  $\tilde{h}(q)$ 

$$\tilde{h}(q) = \frac{1}{\rho^2} \hat{\rho}_{12}(q) - (2\pi)^d \delta(q) 
= \frac{1}{\rho} e^{-Aq^2} + \int \frac{dk_1}{(2\pi)^d} \frac{dk_2}{(2\pi)^d} e^{-Ak_1(k_1 - q)} e^{-Ak_2(k_2 - q)} e^{-Aq^2} \hat{g}_{liq}(k_1) \hat{g}_{liq}(k_2) \hat{q}_A^{-1}(q - k_1 - k_2) - (2\pi)^d \delta(q) 
= e^{-Aq^2} \left[ \frac{1}{\rho} + \int \frac{dk_1}{(2\pi)^d} e^{-Ak_1(k_1 - q)} \hat{h}_{liq}(k_1) \int \frac{dk_2}{(2\pi)^d} e^{-Ak_2(k_2 - q)} \hat{h}_{liq}(k_2) \hat{q}_A^{-1}(q - k_1 - k_2) \right] 
+ 2 \int \frac{dk}{(2\pi)^d} e^{-Ak(k - q)} \hat{h}_{liq}(k) \hat{q}_A^{-1}(q - k) + \hat{q}_A^{-1}(q) - (2\pi)^d \delta(q) \right]$$
(4.0.19)

The non-ergodicity factor expression is thus

$$f(q) = \frac{\rho \tilde{h}}{S(q)} = \frac{e^{-Aq^2}}{1 + \rho h(q)} \left[ 1 + \rho \int \frac{dk_1}{(2\pi)^d} e^{-Ak_1(k_1 - q)} \hat{h}_{liq}(k_1) \int \frac{dk_2}{(2\pi)^d} e^{-Ak_2(k_2 - q)} \hat{h}_{liq}(k_2) \hat{q}_A^{-1}(q - k_1 - k_2) \right]$$

$$+ 2 \int \frac{dk}{(2\pi)^d} e^{-Ak(k - q)} \hat{h}_{liq}(k) \hat{q}_A^{-1}(q - k) + Q_A(q)$$

$$(4.0.20)$$

where 
$$Q_A(q) = \hat{q}_A^{-1}(q) - (2\pi)^d \delta(q) = \int dr \frac{q_A(r) - 1}{q_A(r)} e^{iqr}$$
 (4.0.21)

The  $q_A$  function is a positive function which converges through 1, which gives us the possibility of the convergence of the integral, and it is bigger than its value at 0

$$q_A(0) = \frac{1}{\Gamma(d/2)} \int_0^\infty dr g_{liq}(\sqrt{4Ar}) r^{d/2-1} e^{-r}$$
(4.0.22)

which creates some numerical problems if A is too small,  $q_A(0)$  is null and thus, we cannot compute  $Q_A(r)$ .

# Conclusion

In the approach we developed, we can derive the phase diagram of the glass transition in whatever dimension, using a perturbation around the infinite dimension solution. This work is coherent with the previous results developed at infinite dimension, in the small cage expansion and with the simulations results. We have still some possible improvement in our results: we should find a better generalization of the Verlet-Weis (VW) approximation in an arbitrary dimension, using the techniques which are used in the dimension 3 and a better Bessel function algorithm should be realized to have good results for the Kauzmann transition. Moreover, the simulation of the non-ergodicity factor should be realized.

# Acknowledgments

For his help all along the internship, in particular during written calculations where I have some doubts and to solve some programmation errors, I want to thanks F. Zamponi and overall for his explanations about the concepts, not everytime easy to be understand and also for the read-through of this report. I want also to thanks A. Ikeda for his Fortran code of pair correlation and his comments, which helps me and be essential to write our codes.

# References

- [BB11] Ludovic Berthier and Giulio Biroli. Theoretical perspective on the glass transition and amorphous materials. Reviews of Modern Physics, volume 83, pages 587–645, June 2011. arxiv:1011.2578.
- [Cav09] Andrea Cavagna. Supercooled liquids for pedestrian. Physics Reports, volume 476, pages 51–124, March 2009. arxiv:0903.4264.
- [CIPZ11] Patrick Charbonneau, Atsushi Ikeda, Giorgio Parisi, and Francesco Zamponi. Glass transition and random close packing above three dimensions. Physical Review Letters, volume 107, October 2011. arxiv:1107.4666.
- [HM76] JP Hansen and IR MacDonald. Theory of liquids. June 1976.
- [Jac13] Hugo Jacquin. Glass and jamming transition of simple liquids: static and dynamic theory. July 2013. arxiv:1307.3997.
- [MP09] Marc Mézard and Giorgio Parisi. Glasses and replicas. October 2009. arxiv:0910.2838.
- [PZ10] Giorgio Parisi and Francesco Zamponi. Mean field theory of hard sphere glasses and jamming. Reviews of Modern Physics, volume 82, pages 789–845, March 2010. arxiv:0802.2180.
- [SMS89] Yuhua Song, E.A. Mason, and Richard Stratt. Why does the carnahan-starling equation work so well? Journal of Physical Chemistry, April 1989.
- [VW72] Loup Verlet and Jean-Jacques Weis. Perturbation theory for the thermodynamic properties of simple liquids. Molecular Physics, pages 1013–1024, June 1972.